

Exponential Error Suppression for Near-Term Quantum Devices

Bálint Koczor*

Department of Materials, University of Oxford, Parks Road, Oxford OX1 3PH, United Kingdom

As quantum computers mature, quantum error correcting codes (QECs) will be adopted in order to suppress errors to any desired level E at a cost in qubit-count n that is merely poly-logarithmic in $1/E$. However in the NISQ era, the complexity and scale required to adopt even the smallest QEC is prohibitive. Instead, error mitigation techniques have been employed; typically these do not require an increase in qubit-count but cannot provide exponential error suppression. Here we show that, for the crucial case of estimating expectation values of observables (key to almost all NISQ algorithms) one can indeed achieve an effective exponential suppression. We introduce the Error Suppression by Derangement (ESD) approach: by increasing the qubit count by a factor of $n \geq 2$, the error is suppressed exponentially as Q^n where $Q < 1$ is a suppression factor that depends on the entropy of the errors. The ESD approach takes n independently-prepared circuit outputs and applies a controlled derangement operator to create a state whose symmetries prevent erroneous states from contributing to expected values. The approach is therefore ‘NISQ-friendly’ as it is modular in the main computation and requires only a shallow circuit that bridges the n copies immediately prior to measurement. Imperfections in our derangement circuit do degrade performance and therefore we propose an approach to mitigate this effect to arbitrary precision due to the remarkable properties of derangements. a) they decompose into a linear number of elementary gates – limiting the impact of noise b) they are highly resilient to noise and the effect of imperfections on them is (almost) trivial. In numerical simulations validating our approach we confirm error suppression below 10^{-6} for circuits consisting of several hundred noisy gates (two-qubit gate error 0.5%) using no more than $n = 4$ circuit copies.

Introduction—The control of errors, also called noise, is fundamental to the successful exploitation of quantum computers. The powerful and general theory of quantum fault tolerance, exploiting quantum error correcting codes (QECs), provides a theoretical blueprint for controlling errors in the era when quantum devices are large-scale [1–7]. Encoding qubits into collective states permits the suppression of the error rate on *logical* gates to an arbitrary small level at the cost of increasing the number of physical qubits. Below a threshold the error suppression is exponential in the hardware scaling. However, this powerful solution is prohibitive in the current era of noisy, intermediate scale quantum (NISQ) devices for the following reasons [8]. (a) the qubit-count scale factor is at least 5 for the simplest codes that protect against comprehensive noise types [9, 10]. (b) the extra circuit complexity that is needed in order to monitor the stabilisers, or equivalent measures of code integrity, is very considerable and will boost the effective error rate. (c) in order to achieve a universal set of quantum operations on code-protected logical qubits, highly-non-trivial additional measures such as magic state purification must be undertaken, greatly increasing the hardware scale.

Here we present an approach to controlling errors that achieves the key benefit of true QEC in the specific (but pivotal) case of estimating expected values of operators, and does so without the three key drawbacks of QEC mentioned above. The present idea requires an increased qubit-count (by some integer factor that is at least two), and therefore it is more hardware-expensive

than many NISQ error mitigation schemes [11–19], but in return it provides exponential error suppression – which other NISQ solutions cannot. Therefore the approach might be seen as sitting between the established NISQ-era techniques and the full QEC domain, albeit nearer to the NISQ approaches. Moreover the present approach is compatible with other NISQ mitigation techniques such as extrapolation, quasi-probability or symmetry verification [11–18]; In fact, extrapolation is used in the present analysis to negate the impact of errors in the derangement process.

Estimating expectation values on a quantum device is of central importance and most near-term applications do need to estimate such expectation values. Many variants of the so-called variational quantum eigensolver have been proposed for solving classically intractable problems, such as simulating quantum systems described by Hamiltonians \mathcal{H} [11, 12, 14, 20–40]. Expectation values of Hamiltonian operators are typically decomposed as $\langle \psi | \mathcal{H} | \psi \rangle = \sum_k c_k \langle \psi | P_k | \psi \rangle$, where P_k are tensor products of Pauli operators, and we will collectively denote them as $\sigma \equiv P_k$ in the following. Various approaches have been proposed for estimating such expectation values $\langle \psi | \sigma | \psi \rangle$ using quantum computers [11, 12, 41–43]. However, without comprehensive error correction, errors during the state preparation will contribute a bias as $\langle \psi_k | \sigma | \psi_k \rangle$ into the result, where $|\psi_k\rangle$ are erroneous states as shown in the next section. There exist numerous error mitigation techniques that potentially reduce the effect of such contributions without increasing the number N of qubits, but at the cost of a significantly increased number of measurements and increased numbers of circuit variants [11–18].

* balint.koczor@materials.ox.ac.uk

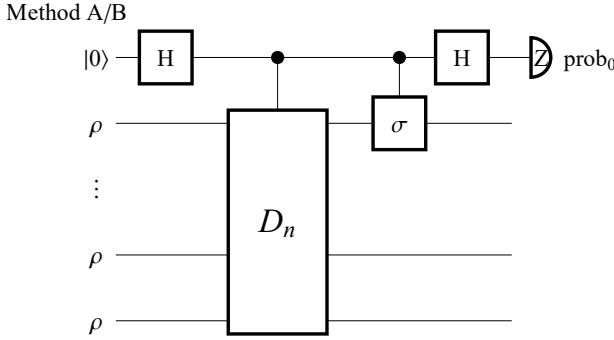


FIG. 1. A possible implementation of the ESD approach. Our derangement operator D_n is a generalisation of the SWAP operator and acts on n (not necessarily identical) copies of the quantum state $\rho = \lambda|\psi\rangle\langle\psi| + (1-\lambda)\rho_{\text{err}}$. In the above circuit D_n permutes the n registers and allows only permutation symmetric combinations, e.g., $|\psi\rangle^{\otimes n}$, to contribute to the expectation-value measurement process. The probability of measuring the ancilla qubit in the 0 state enables us to approximate the the ideal expectation value $\langle\psi|\sigma|\psi\rangle$ and errors are suppressed exponentially in n . This derangement operator can be implemented as a shallow circuit using a linear number $N(n-1)$ of primitive, controlled, two-qubit SWAP gates.

Here we take a different route and introduce the Error Suppression by Derangement (ESD) approach: we introduce a high degree of symmetry by preparing n copies of the quantum state $|\psi\rangle$ and use derangement operators (generalised SWAP operations) to protect collective permutation symmetry. Most noise events that occur during the imperfect preparation of $|\psi\rangle$ break this permutation symmetry and they are effectively ‘filtered out’ by the ESD. We outline a possible construction for such a measurement process in Fig. 1 and thoroughly analyse its properties while supporting our claims with rigorous mathematical proofs.

Our construction is certainly very well suited for NISQ hardware for the following reasons. First, the main computation is modular as the n copies of the computational state are prepared completely independently. Second, the derangement circuit that ‘bridges’ the n copies immediately prior to measurements is sufficiently shallow (as it can be decomposed into a linear number of primitive gates) and therefore picks up significantly less noise than the state-preparation stage. Third, the derangement measurement is highly resilient to noise, since most error events that occur during the derangement process do not contribute to the result. Let us now introduce basic concepts and explain the main idea in detail.

Noisy quantum states and entropies—Near-term quantum devices aim to prepare computational quantum states $|\psi\rangle$ for, e.g., simulating other quantum systems or beyond. These quantum devices are, however, imperfect and can only prepare noisy, mixed quantum states which we model via the following spectral decomposition

of a density matrix

$$\rho = \lambda|\psi\rangle\langle\psi| + (1-\lambda)\sum_{k=2}^{2^N} p_k|\psi_k\rangle\langle\psi_k|. \quad (1)$$

Here $\lambda \leq 1$ and $\sum_k p_k = 1$ is an error probability distribution. Our principal assumption, the only one that we need to make, is that there is a dominant eigenvector $|\psi\rangle$ in the state ρ that approximates the ideal, desired computational state. Indeed, this is only an approximation in general since coherent errors might occur during the preparation of ρ : Even when the error model is purely incoherent, a small coherent mismatch in the dominant eigenvector can be expected, refer to later text and to Sec. C1. We prove elsewhere general upper bounds on this coherent mismatch that decay exponentially with the entropy of the error distributions (quadratically with the largest error probability) [44] and we remark here that many applications, including variational algorithms, are inherently robust to such coherent errors.

We further stress that in principle λ can be arbitrarily small, e.g., $\lambda = 10^{-6}$, as long as it is the dominant component and larger than any other eigenvalue as $\lambda > (1-\lambda)p_k$ for all k . Although, for extremely low λ other factors such as the sampling cost may of course become prohibitive in practice as we discuss in later text.

Furthermore, p_k are probabilities of erroneous contributions $|\psi_k\rangle$, and we will refer to these (orthonormal) states as ‘error events’ in the following and we denote their probability vector as \underline{p} . To keep our discussion completely general we do not restrict the probability distribution \underline{p} at all, but we remark that Rényi entropies [45] as

$$H_n(\underline{p}) := \frac{1}{1-n} \ln \left[\sum_{k=2}^{2^N} p_k^n \right]$$

will have a crucial effect on our results and, indeed, for typical experimental quantum systems one can expect that $H_n(\underline{p})$ are large.

Main idea—As discussed above, most applications targeting early quantum devices aim to estimate expectation values of the form $\langle\psi|\sigma|\psi\rangle$, but errors during state preparation contribute bias $\langle\psi_k|\sigma|\psi_k\rangle$ to the estimated expectation values. Here we aim to suppress these contributions via the following novel principle. Let us prepare n copies of the state ρ from Eq. (1). The most likely event is that no error happens during state preparation: with a probability λ^n the resulting state (immediately after state preparation) is $|\psi, \psi, \dots, \psi\rangle$. Measuring the expectation value *on the first register* gives the desired result $\langle\psi, \dots, \psi, \psi|\sigma|\psi, \psi, \dots, \psi\rangle = \langle\psi|\sigma|\psi\rangle$.

The second most likely event is that an error happens to one of the registers, for example the first register, mapping its state to the orthogonal eigenvector in the density matrix $|\psi_k\rangle$; A measurement then returns the error term $\langle\psi_k, \dots, \psi, \psi|\sigma|\psi_k, \psi, \dots, \psi\rangle = \langle\psi_k|\sigma|\psi_k\rangle$. However, if one instead measures the expectation value of the product

σSWAP_{1n} , where SWAP_{1n} swaps the registers 1 and n , we then obtain

$$\langle \psi_k, \dots \psi, \psi | \sigma \psi, \psi, \dots \psi_k \rangle = \langle \psi_k | \sigma | \psi \rangle \langle \psi_k | \psi \rangle = 0.$$

Here the SWAP operator changed the ordering of the registers as $|\psi_k, \psi, \dots \psi\rangle \rightarrow |\psi, \psi, \dots \psi_k\rangle$ and the result is 0 due to the orthogonality of the eigenvectors of the density matrix. We can straightforwardly generalise this idea to the case where all registers are swapped, allowing only permutation-symmetric states to contribute to the measurement of expectation values. We will refer to this permutation operation as ‘derangement’. While one can certainly realise the above measurement principle in various different ways, we propose one such circuit in Fig. 1. We rigorously prove properties of this particular construction in Result 1, Result 2 and Result 3, but we stress that the current proposal is not limited to the circuit in Fig. 1 (and even Fig. 1 leaves room for various different physical implementations which we discuss in later text).

Exponential error suppression—The circuit in Fig. 1 can be thought of as a Hadamard-test technique [1] that measures the expectation value of the product σD_n , where the derangement operator D_n permutes the n input registers; as we will explain in a later section and discuss that it only requires a linear number of primitive gates to construct. We prove in Theorem 1 that only permutation-symmetric combinations can pass through the derangement measurement in Fig. 1, such as the error-free state $|\psi\rangle^{\otimes n}$ (which happens with a probability λ^n) or states in which the same errors occurred to all registers $|\psi_k\rangle^{\otimes n}$ (which happen with probabilities $(1-\lambda)^n p_k^n$). Our general result in Theorem 1 determines the probability prob_0 of measuring the ancilla qubit in Fig. 1 in the 0 state as

$$\begin{aligned} 2\text{prob}_0 - 1 &= \text{Tr}[\rho^n \sigma] \\ &= \lambda^n \langle \psi | \sigma | \psi \rangle + (1-\lambda)^n \sum_{k=2}^{2^n} p_k^n \langle \psi_k | \sigma | \psi_k \rangle, \end{aligned}$$

where the erroneous contributions $\langle \psi_k | \sigma | \psi_k \rangle$ are exponentially suppressed as we increase n .

Dividing by λ^n allows one to approximate the expectation value of a unitary observable $\sigma^2 = \text{Id}$, or otherwise the real part of the expected value of a unitary operator. We work out two explicit results in Example 1 and Example 2 that demonstrate how the above scheme allows to exponentially suppress the noise as we increase the number n of copies of ρ and how its efficacy depends on properties of the probability distribution p_k . Let us now state approximation errors of Methods A and B.

Result 1. *Let us prepare n identical copies of the experimental quantum state ρ from Eq. (1) and apply the derangement measurement from Fig. 1. Both Methods A and B approximate the expectation value $\langle \psi | \sigma | \psi \rangle$ by estimating prob_0 on the ancilla qubit. Method B only*

estimates prob_0 and assumes explicit knowledge of the dominant eigenvalue λ . In Method A we additionally estimate prob'_0 by repeating the procedure but omitting the controlled- σ gate in Fig. 1. We denote their approximation errors as \mathcal{E}_A and \mathcal{E}_B , respectively,

$$\text{Method A: } \frac{2\text{prob}_0 - 1}{2\text{prob}'_0 - 1} = \langle \psi | \sigma | \psi \rangle + \mathcal{E}_A, \quad (2)$$

$$\text{Method B: } \frac{2\text{prob}_0 - 1}{\lambda^n} = \langle \psi | \sigma | \psi \rangle + \mathcal{E}_B, \quad (3)$$

and these approximation errors generally decay exponentially with the number n of copies via the sequence Q_n

$$|\mathcal{E}_A| \leq \frac{2Q_n}{1+Q_n} \quad \text{and} \quad |\mathcal{E}_B| \leq Q_n, \quad (4)$$

which is bounded $Q_n \leq \text{const} \times Q^n$ via the suppression factor $Q < 1$ as established in Theorem 2 and in Lemma 1.

We show in Lemma 1 that the errors also decay exponentially with the Rényi entropy $H_n(p)$ of the error probability distribution from Eq. (1) via $Q_n = (\lambda^{-1}-1)^n \exp[(1-n)H_n(p)]$. Even without knowing or having a good guess of the Rényi entropy of the error probabilities, we can state a general upper bound that only depends on the two largest eigenvalues of the state as $Q_n \leq (\lambda^{-1}-1)^n (p_{\max})^{n-1}$, where p_{\max} is the largest of the error probabilities p_k in Eq. (1)

Numerical simulations—We consider a 12-qubit quantum state that is produced by a noisy, parametrised quantum circuit typically used in variational quantum algorithms – our circuit consists of 10 alternating layers and overall 372 quantum gates. Refer to Sec. E for more details. Each two-qubit gate undergoes 2-qubit depolarising noise with 0.5% probability and each single-qubit gate undergoes depolarising noise with 0.05% probability. The resulting state has a dominant eigenvalue $\lambda \approx 0.51$ and it has a high entropy, full-rank error probability distribution via the Rényi entropies that monotonically decrease with n as $H_2(p) = 4.69$, $H_3(p) = 4.38$, $H_4(p) = 4.23$, and $H_\infty(p) = 3.63$. Refer to Sec. E for more details.

We remark that despite the purely incoherent error model, the dominant eigenvector $|\psi\rangle$ of ρ is slightly different than what one would obtain from a completely error-free computation and in the plots we compute errors using the dominant eigenvector, refer to Sec. E for more details. Nevertheless, the effect of such a coherent mismatch becomes negligible for large systems (see Sec. C 1) and we discuss generally the effect of coherent errors in later text.

In Fig. 2 a) we plot our error suppression upper bounds from Result 1, i.e., solid lines represent the error bounds computed from the Rényi entropy of the quantum state’s error-probability distribution and dashed lines represent the general upper bound $Q_n \leq (\lambda^{-1}-1)^n (p_{\max})^{n-1}$ where the largest error probability is $p_{\max} = 0.026$ and the suppression factor is $Q = 0.026$. Red and blue colours correspond to Method A and Method B, respectively. We

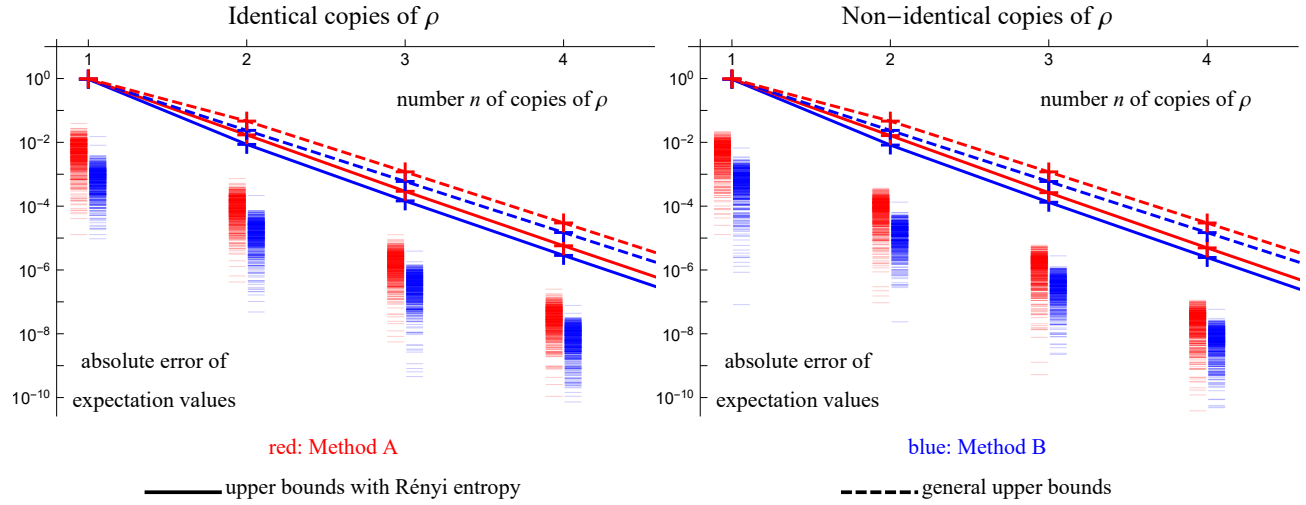


FIG. 2. Simulation of a 12-qubit state with 372 noisy quantum gates. Errors in estimating the ideal expectation value $\langle \psi | \sigma | \psi \rangle$ decay exponentially with the number of copies n of the quantum state ρ . Dashed lines: our general upper bounds on the errors from Result 1 and Result 2 only require the knowledge of the dominant eigenvalue λ and the largest error probability p_{max} from Eq. (1). Solid lines: our upper bounds based on the Rényi entropy of the quantum states. Red and blue bars: approximation errors obtained with 500 randomly selected Pauli strings (observables σ) are significantly below the upper bounds. a) all copies of ρ are perfectly identical and b) all copies of ρ are significantly different (but they commute as this case can be simulated efficiently) and their trace distance is 0.01 due to their different eigenvalue distributions.

have generated 500 Pauli strings as observables randomly and computed the errors in estimating their expectation values (there are overall $4^{12} = 1.68 \times 10^7$ Pauli strings, and we randomly select 500). These samples (see horizontal lines in Fig. 2) are significantly below our upper bounds and seem to decrease in a similar exponential order as our bounds (i.e., slope is similar in the logarithmic plot).

Method B slightly outperforms Method A (slightly smaller errors as blue is slightly below red), but it requires an exact (or very precise) knowledge of the dominant eigenvalue λ . Nevertheless, this eigenvalue could be determined precisely by existing approaches in special cases, e.g., as in [46].

Effect of non-identical states—We now turn to the question of how the efficacy of our error suppression scheme is affected when the n copies of the state ρ are not identical.

Result 2. *We assume that all copies of the quantum state are arbitrarily different via $\rho_1 \neq \rho_2 \neq \dots \neq \rho_n$ except that their dominant eigenvector is $|\psi\rangle$. Our scheme via Lemma 3 still provides exponentially decreasing approximation errors when the dominant eigenvalue of the worst quality copy is $\lambda_{\min} > 1/2$ via*

$$\text{Method A: } \frac{2\text{prob}_0 - 1}{2\text{prob}'_0 - 1} = \langle \psi | \sigma | \psi \rangle + \mathcal{O}([\lambda_{\min}^{-1} - 1]^n), \quad (5)$$

$$\text{Method B: } \frac{2\text{prob}_0 - 1}{\prod_{\mu=1}^n \lambda_\mu} = \langle \psi | \sigma | \psi \rangle + \mathcal{O}([\lambda_{\min}^{-1} - 1]^n). \quad (6)$$

In the special case when all copies of the quantum state commute (same eigenvectors but different eigenvalues)

one can expect very similar approximation errors to Result 1 via an effective suppression rate Q_n^{eff} .

We can efficiently simulate the case when all copies of the quantum state commute. We disturbed every copy of the density matrix such that their trace distance is $\|\rho_k - \rho_l\| \approx 10^{-2}$ for all $k \neq l$. Note that the approximation errors in Fig. 2 b) are very similar to Fig. 2 a) and they are approximately upper bounded by the same upper bounds from Result 1 (as expected from Lemma 3).

Complexity analysis—Let us now analyse resource requirements of our ESD approach. In particular, one needs to prepare a suitable number n of copies of ρ in order to suppress its errors below a threshold level, that we will refer to as precision and denote as \mathcal{E} . The overall number of qubits required is then $nN+1$, where N is the number of qubits in the computational state ρ . Furthermore, one needs to repeat measurements many times to sufficiently reduce the effect of so-called shot noise, i.e., we estimate the probability only from a finite number of repetitions [47]. We denote the number of repetitions as N_s . Let us now summarise our general results from Lemma 2.

Result 3. *In order to reach a precision \mathcal{E} in determining the expectation value $\langle \psi | \sigma | \psi \rangle$, one requires a logarithmic number $n = \mathcal{O}(\ln \mathcal{E}^{-1} / \ln Q^{-1})$ of copies of the quantum state ρ (up to rounding). Here $Q < 1$ is the suppression factor from Result 1 that depends on Rényi entropies. The number N_s of measurements required to suppress shot noise below the threshold \mathcal{E} grows poly-*

mially as

$$\begin{aligned} \text{Method A: } N_s &= \mathcal{O}[\mathcal{E}^{-2(1+2f)}], \\ \text{Method B: } N_s &= \mathcal{O}[\mathcal{E}^{-2(1+f)}], \end{aligned}$$

where $f = \ln[\lambda^{-1}/\ln Q^{-1}]$ increases the polynomial order compared to the standard shot-noise limit $\mathcal{O}(\mathcal{E}^{-2})$ and we have derived a general upper bound on f in Lemma 2.

Dividing by the exponentially attenuated factor λ^n in both Methods A and B, in Result 1 requires an increasingly large number of measurements to sufficiently suppress shot noise. Methods A and B are therefore less efficient than permitted by the standard shot noise limit $N_s = \mathcal{O}(\mathcal{E}^{-2})$. For example in the extreme, but still valid, case of $\lambda = 10^{-6}$ and $Q = 1/2$ we obtain $f = 19.9$ which increases the sampling costs prohibitively in practice. Nevertheless, the polynomial order of $\mathcal{O}(\mathcal{E}^{-1})$ is only logarithmically increased via f and its effect might be negligible in practically relevant scenarios. For example in our simulations in Fig. 2 we obtain $f = 0.18$ using our expression $Q = (\lambda^{-1}-1)p_{\max}$ in Lemma 1. Indeed, we recover the standard shot-noise limit $\mathcal{O}(\mathcal{E}^{-2})$ for very good quality states $\lambda \approx 1$ or for very high entropy probabilities.

In summary, the complexity of our ESD approach only depends on the largest eigenvalue λ of the state and on the suppression factor Q from Result 1 – which is determined by the Rényi entropy of the error probabilities. As expected, the number N_s of samples grows polynomially with the target precision \mathcal{E}^{-1} and the system size grows logarithmically with \mathcal{E}^{-1} . Let us remark that in case of certain applications a global prefactor in observable expectation values does not matter – such as in case of VQE – and one can use method B but omitting the division by λ^n . Using Method B significantly reduces the measurement costs and reduces errors from Result 1 when compared to Method A. Let us now discuss the gate count of our approach which grows linearly with the system size n and N .

Derangements of quantum registers—Our ESD circuit in Fig. 1 uses a generalisation of the SWAP operator that permutes subspaces of quantum registers. Recall that in general there exist $n!$ permutations of a set of n ordered elements. Derangements are a subset of the collection of all permutations: they permute the n elements such that no element remains in place [48, 49]. We define D_n as unitary representations of derangements that permute subspaces of n quantum registers in Definition 1. For example, for $n = 2$ our D_2 reduces to the usual SWAP operator as

$$D_2|\psi_1, \psi_2\rangle = \text{SWAP}_{12}|\psi_1, \psi_2\rangle = |\psi_2, \psi_1\rangle. \quad (7)$$

For $n = 3$ we have two distinct constructions for possible D_3 derangement operators as

$$\begin{aligned} \text{SWAP}_{13} \text{SWAP}_{12}|\psi_1, \psi_2, \psi_3\rangle &= |\psi_3, \psi_1, \psi_2\rangle, \\ \text{SWAP}_{23} \text{SWAP}_{12}|\psi_1, \psi_2, \psi_3\rangle &= |\psi_2, \psi_3, \psi_1\rangle. \end{aligned}$$

For $n = 4$ one has 6 possibilities while in general there are $(n-1)!$ possibilities for constructing distinct derangement operators – but choosing any one of these constructions is sufficient for our scheme to work. Indeed, one could construct derangements D_n straightforwardly as cyclic shifts [50], but the large number of possibilities might offer more preferable constructions that take into account, e.g., hardware constraints such as connectivity. In fact, the large number of invariants could also be used to further reduce our error bounds in Result 2 the following way. By randomly sampling from equivalent derangement operators one could effectively randomise the non-identical input density matrices thereby creating an ‘average’ density matrix. Furthermore, the σ gate in Fig. 1 can be applied to any of the registers further increasing the number of invariants.

Regarding gate complexity, derangement operators can be implemented efficiently in general using $N(n-1)$ primitive controlled two-qubit SWAP gates, where N is the number of qubits in the register $|\psi\rangle$ and n is the number of copies of $|\psi\rangle$. These minimal SWAP circuits (which optimally implement derangement operators) can be constructed by mapping the corresponding permutations to graph trees [51], refer to Definition 1. In conclusion, the depth of the derangement measurement circuit can be expected to be negligible compared to the complexity of preparing the state $|\psi\rangle$.

Mitigating experimental imperfections—So far we have assumed that the derangement operator in Fig. 1 is perfect. Indeed, gates involved here are expected to be noisy in a realistic scenario which ultimately limits the precision of our approach and increases its complexity.

We show in Example 3 quite generally that the derangement operator is highly resilient to experimental imperfections and protects permutation symmetry even under experimental noise. This is nicely illustrated in our simulated noisy circuit: the unmitigated errors in determining prob_0 in Fig. 3 are quite low and are below 10^{-2} for all 50 randomly selected states. The simulated circuit consist of 13 qubits, i.e., 3 copies of a 4 qubit state, and elementary controlled-SWAP gates undergo 3-qubit depolarisations with a probability 3×10^{-3} . Refer to Sec. E for more details

Most importantly, we show in Example 3 quite generally that most errors that occur during the derangement measurement will only trivially affect the final result by (almost) linearly attenuating the output probability prob_0 which can (almost) completely be corrected by an extrapolation. We use extrapolation techniques [11–15, 52] which typically estimate $\text{prob}_0(\epsilon)$ at different values of ϵ and extrapolate, e.g., linearly, to zero noise $\epsilon = 0$. Due to the high degree of noise resilience of the derangement operator, the measurement probabilities $\text{prob}_0(\epsilon)$ are closely approximated by a linear function in ϵ and Fig. 3 illustrates that indeed a linear extrapolation surprisingly well approximates the ideal probability with errors less than 10^{-4} .

Here we aim to suppress errors arbitrarily by account-

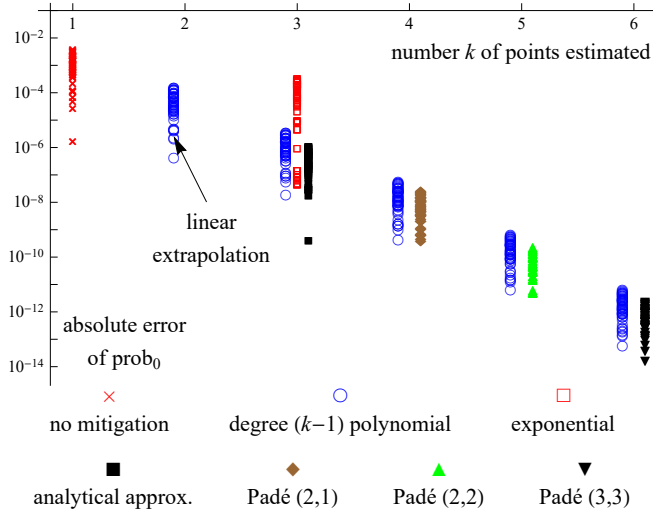


FIG. 3. Mitigating errors in the derangement operator. Extrapolation errors using various different fitting techniques vs. the number of fitting points for 50 randomly selected ansatz states. Elementary gates in the derangement operator in Fig. 1 have an error rate $\epsilon = 10^{-3}$ and an experimentalist can increase this error in $k = 2, 3, 4, \dots$ steps up to $\epsilon = 10^{-2}$. The probability prob_0 from Fig. 1 at $\epsilon = 0$ is estimated by extrapolating to $\epsilon = 0$. The derangement measurement is highly resilient to imperfections (see text) and $\text{prob}_0(\epsilon)$ is almost linear in ϵ . Increasing the degree of the fitting polynomial (blue circles) reduces the extrapolation error exponentially.

ing for the slight non-linearity of the function $\text{prob}_0(\epsilon)$. We prove in Theorem 3 quite generally that expectation values are *exactly* described by degree- ν polynomials as $\text{prob}_0(\epsilon) = \sum_{k=0}^{\nu} c_k \epsilon^k$ and ν is the number of noisy gates. It follows that one can efficiently and exactly determine the ideal probability by determining $\text{prob}_0(\epsilon)$ at $\nu + 1$ different values of ϵ and fitting a degree ν polynomial. Fig. 3 (blue circles) demonstrates how the extrapolation error decreases exponentially with the degree of the fitted polynomial.

Furthermore, we analytically solve the dependence on ϵ in the limiting case of a large number of gates and obtain the approximation

$$\text{prob}_0(\epsilon) \approx \text{prob}_0 - \tilde{\eta} \epsilon \frac{(1-\epsilon)^\nu}{2\epsilon-1} \approx \frac{a_1 \epsilon + a_2 \epsilon^2 + a_3 \epsilon^3}{1 + a_4 \epsilon + a_5 \epsilon^2},$$

where $\tilde{\eta}$ is a constant. The above (3, 3) Padé approximation of the analytical dependence can be determined by fitting the coefficients a_1, a_2, a_3, a_4, a_5 . These Padé approximations appear to slightly outperform degree- k polynomial extrapolations in Fig. 3. Refer to Theorem 3 for more details.

In summary, guided by analytical arguments in Example 3 we propose an efficient and straightforward approach to mitigate experimental errors that occur during the derangement circuit. Determining a degree- k polynomial requires only a linear (in the degree k) measurement overhead when compared to Result 3 while it can dras-

tically reduce the impact of errors. Note, however, that for an increasing number of qubits the noise in the constituent gates accumulates and might significantly attenuate the output probability prob_0 – estimating this attenuated probability to a sufficiently high (relative) precision would require a crucially large number of measurements. In fact, our argument here relies on the assumption that the number of gates is bounded and their errors are sufficiently low so that the output probabilities are not attenuated below a threshold (that ultimately upper bounds the sampling cost). For example, a factor of 0.1 attenuation threshold could be approximated via the formula $0.1 = (1 - \epsilon)^{N(n-1)}$, and at a gate error $\epsilon = 10^{-3}$ it limits the maximal number of qubits as $N(n-1) \leq 2301$ – which is still an encouraging figure in practice. We note that other error mitigation schemes could also be applied straightforwardly to address errors happening during the derangement measurement.

Limitations of our scheme—There is one main limitation of our scheme that we have so far neglected: We assumed that we can prepare a noisy state whose dominant eigenvector is guaranteed to be $|\psi\rangle$. In a realistic experiment one can expect coherent errors such that the dominant eigenvector is $\sqrt{1-c}|\psi\rangle + \sqrt{c}|\psi_{\text{err}}\rangle$. We discuss that even incoherent noise channels can result in such a coherent mismatch (although potentially negligible for large systems and can be mitigated straightforwardly) in Sec. C1. As opposed to error correcting schemes, our ESD approach is completely oblivious to these discrepancies and ultimately such errors will limit the precision. Nevertheless, well-established techniques enable us to suppress these coherent errors, e.g., via converting them into incoherent errors by Pauli twirling [53–56]. Furthermore, in the context of variational algorithms one could slightly re-adjust variational parameters such that the overlaps between copies $\text{Tr}[\rho_k \rho_l]$ are maximal for every $k \neq l$ – note that measuring such overlaps is possible with the setup in Fig. 1. This ensures us that the dominant eigenvector of every copy is (close to) identical and a global coherent mismatch will anyway not effect a variational optimisation problem, such as VQE. One could also use Clifford circuits to calibrate or validate the quantum device by comparing to expectation values obtained from (efficient) classical simulations [16, 17].

We further remark that we have also neglected the effect of measurement errors, i.e., when the probability of collapsing into state 0 is biased. Nevertheless, there exist well-established techniques for mitigating the effect of such imperfections.

Discussion and Conclusion—This work has introduced a novel principle for suppressing errors in near term quantum devices. As opposed to error mitigation techniques, our ESD approach requires an increased system size: By preparing n identical copies of a computational state, our derangement circuit protects its permutation symmetry and suppresses errors in an expectation value measurement exponentially (in the number n of copies). Furthermore, ESD is very NISQ friendly, since the n copies of the

computational state can be prepared completely independently and they only need to be ‘bridged’ by a shallow derangement circuit immediately prior to measurement. Another significant advantage of the ESD approach is that it is completely oblivious to the error model during the state preparation process and works (in principle) with arbitrarily high error rates as long as the computational state is the dominant eigenvector in the mixed computational state ρ .

The main limitation of the ESD approach is that it cannot address coherent noise or a coherent mismatch in the dominant eigenvector, although the impact of such errors could be reduced significantly via well-established techniques. As long as the derangement circuit is assumed to be perfect, the sample complexity of our ESD approach is polynomial and comparable to the standard shot-noise limit in practically relevant scenarios. However, errors during the derangement process do degrade the performance of the present approach and one needs to rely on error mitigation techniques to reduce this impact. Since such error mitigation techniques generally introduce a significant measurement overhead (exponential in the number of gates), the ESD approach is ultimately limited by errors affecting the shallow derangement circuit. However, our analytical arguments and numerical experiments validate that in practically relevant scenarios (e.g., up to ≈ 2000 qubits) the introduced measurement overhead is reasonable.

Let us now briefly comment on prior approaches that similarly consider identical copies of quantum states and similarly apply SWAP operators (or generalisations of them). In fact, numerous prior works have considered and exploited the permutation symmetry of identical copies of mixed states in the context of, e.g., reconstructing spectral properties of mixed quantum states [50, 57–62], probing their entanglement characteristics [63–65], for constructing universal quantum software [66], and for optimal state discrimination [67–69]. Indeed, in the special case of $n = 2$ copies, our scheme is comparable to a modification of the usual SWAP-test circuit [50]. However, as opposed to previous works, here we are not interested in the input mixed state ρ , but only in its dominant eigenvector $|\psi\rangle$ that represents a computational quantum state. In fact, we regard any other contribution in the state ρ as ‘noise’ which we aim to exclude from the

expectation-value measurement process. The present approach could also be compared to entanglement distillation protocols [70–72], however, our derangement circuit cannot exponentially improve the ‘quality’ of the input states, but only exclude erroneous contributions from the expectation-value measurement process.

Let us finally remark that the ESD approach leaves a lot of room for a large number of different physical implementations, beyond the circuit in Fig.1 that has been analysed in detail in this work. Our circuit in Fig.1 is only one possible realisation of the general principle outlined here and even this circuit has a large number of invariants, e.g., $!n$ different derangement operators. We only need to remark here that the results presented here are very general, and our example circuit could certainly be improved by combining it with advanced techniques for example, by simultaneously measuring groups of commuting observables [42, 43] – but we expect these can only introduce constant factor improvements and will not change the main results in this work. As such, one natural extension would be to investigate the case when setting $\sigma = \text{Id}$ and post-selecting the ancilla qubit – effectively projecting the computational state onto a subspace that is closer to permutation symmetric combinations. In future work we will explore the numerous possibilities offered by the general principle introduced here.

ACKNOWLEDGMENTS

I would like to thank Simon C. Benjamin for his invaluable comments and challenging questions. His help and support was crucial for finalising this work. I would like to thank Earl Campbell, Robert Zeier, Suguru Endo and Ying Li for their very constructive and valuable comments on drafts of this work. I acknowledge funding received from EU H2020-FETFLAG-03-2018 under the grant agreement No 820495 (AQTON). The numerical modelling involved in this study made use of the Quantum Exact Simulation Toolkit (QuEST), and the recent development QuESTlink [73] which permits the user to use Mathematica as the integrated front end. I am grateful to those who have contributed to both these valuable tools.

[1] M. A. Nielsen and I. L. Chuang, *Quantum Computation and Quantum Information*, 10th ed. (Cambridge University Press, New York, NY, USA, 2011).

[2] D. A. Lidar and T. A. Brun, *Quantum error correction* (Cambridge university press, 2013).

[3] D. Gottesman, Theory of fault-tolerant quantum computation, *Phys. Rev. A* **57**, 127 (1998).

[4] P. W. Shor, Scheme for reducing decoherence in quantum computer memory, *Phys. Rev. A* **52**, R2493 (1995).

[5] A. R. Calderbank and P. W. Shor, Good quantum error-correcting codes exist, *Phys. Rev. A* **54**, 1098 (1996).

[6] E. Knill, R. Laflamme, and W. H. Zurek, Resilient quantum computation, *Science* **279**, 342 (1998).

[7] D. Aharonov and M. Ben-Or, Fault-Tolerant Quantum Computation with Constant Error, in *Proceedings of the Twenty-Ninth Annual ACM Symposium on Theory of Computing*, STOC '97 (Association for Computing Machinery, New York, NY, USA, 1997) p. 176–188.

- [8] J. Preskill, Quantum Computing in the NISQ era and beyond, arXiv preprint arXiv:1801.00862 (2018).
- [9] R. Laflamme, C. Miquel, J. P. Paz, and W. H. Zurek, Perfect Quantum Error Correcting Code, *Phys. Rev. Lett.* **77**, 198 (1996).
- [10] C. H. Bennett, D. P. DiVincenzo, J. A. Smolin, and W. K. Wootters, Mixed-state entanglement and quantum error correction, *Phys. Rev. A* **54**, 3824 (1996).
- [11] S. Endo, Z. Cai, S. C. Benjamin, and X. Yuan, Hybrid quantum-classical algorithms and quantum error mitigation, arXiv preprint arXiv:2011.01382 (2020).
- [12] Y. Li and S. C. Benjamin, Efficient Variational Quantum Simulator Incorporating Active Error Minimization, *Phys. Rev. X* **7**, 021050 (2017).
- [13] S. Endo, S. C. Benjamin, and Y. Li, Practical Quantum Error Mitigation for Near-Future Applications, *Phys. Rev. X* **8**, 031027 (2018).
- [14] A. Kandala, K. Temme, A. D. Córcoles, A. Mezzacapo, J. M. Chow, and J. M. Gambetta, Error mitigation extends the computational reach of a noisy quantum processor, *Nature* **567**, 491 (2019).
- [15] K. Temme, S. Bravyi, and J. M. Gambetta, Error Mitigation for Short-Depth Quantum Circuits, *Phys. Rev. Lett.* **119**, 180509 (2017).
- [16] A. Strikis, D. Qin, Y. Chen, S. C. Benjamin, and Y. Li, Learning-based quantum error mitigation, arXiv preprint arXiv:2005.07601 (2020).
- [17] P. Czarnik, A. Arrasmith, P. J. Coles, and L. Cincio, Error mitigation with Clifford quantum-circuit data, arXiv preprint arXiv:2005.10189 (2020).
- [18] S. McArdle, X. Yuan, and S. Benjamin, Error-Mitigated Digital Quantum Simulation, *Phys. Rev. Lett.* **122**, 180501 (2019).
- [19] A. G. Rattew, Y. Sun, P. Minssen, and M. Pistoia, Quantum Simulation of Galton Machines Using Mid-Circuit Measurement and Reuse, arXiv preprint arXiv:2009.06601 (2020).
- [20] E. Farhi, J. Goldstone, and S. Gutmann, A quantum approximate optimization algorithm, arXiv preprint arXiv:1411.4028 (2014).
- [21] A. Peruzzo, J. McClean, P. Shadbolt, M.-H. Yung, Q. Zhou, P. J. Love, A. Aspuru-Guzik, and J. L. O'Brien, A variational eigenvalue solver on a photonic quantum processor, *Nature communications* **5** (2014).
- [22] Y. Wang, F. Dolde, J. Biamonte, R. Babbush, V. Bergholm, S. Yang, I. Jakobi, P. Neumann, A. Aspuru-Guzik, J. D. Whitfield, *et al.*, Quantum simulation of helium hydride cation in a solid-state spin register, *ACS nano* **9**, 7769 (2015).
- [23] P. J. J. O'Malley, R. Babbush, I. D. Kivlichan, J. Romero, J. R. McClean, R. Barends, J. Kelly, P. Roushan, A. Tranter, N. Ding, B. Campbell, Y. Chen, Z. Chen, B. Chiaro, A. Dunsworth, A. G. Fowler, E. Jeffrey, E. Lucero, A. Megrant, J. Y. Mutus, M. Neeley, C. Neill, C. Quintana, D. Sank, A. Vainsencher, J. Wenner, T. C. White, P. V. Coveney, P. J. Love, H. Neven, A. Aspuru-Guzik, and J. M. Martinis, Scalable Quantum Simulation of Molecular Energies, *Phys. Rev. X* **6**, 031007 (2016).
- [24] Y. Shen, X. Zhang, S. Zhang, J.-N. Zhang, M.-H. Yung, and K. Kim, Quantum implementation of the unitary coupled cluster for simulating molecular electronic structure, *Phys. Rev. A* **95**, 020501 (2017).
- [25] J. R. McClean, J. Romero, R. Babbush, and A. Aspuru-Guzik, The theory of variational hybrid quantum-classical algorithms, *New J. Phys.* **18**, 023023 (2016).
- [26] S. Paesani, A. A. Gentile, R. Santagati, J. Wang, N. Wiebe, D. P. Tew, J. L. O'Brien, and M. G. Thompson, Experimental Bayesian Quantum Phase Estimation on a Silicon Photonic Chip, *Phys. Rev. Lett.* **118**, 100503 (2017).
- [27] J. I. Colless, V. V. Ramasesh, D. Dahlen, M. S. Blok, M. E. Kimchi-Schwartz, J. R. McClean, J. Carter, W. A. de Jong, and I. Siddiqi, Computation of Molecular Spectra on a Quantum Processor with an Error-Resilient Algorithm, *Phys. Rev. X* **8**, 011021 (2018).
- [28] R. Santagati, J. Wang, A. A. Gentile, S. Paesani, N. Wiebe, J. R. McClean, S. Morley-Short, P. J. Shadbolt, D. Bonneau, J. W. Silverstone, D. P. Tew, X. Zhou, J. L. O'Brien, and M. G. Thompson, Witnessing eigenstates for quantum simulation of Hamiltonian spectra, *Science Advances* **4**, 10.1126/sciadv.aap9646 (2018).
- [29] A. Kandala, A. Mezzacapo, K. Temme, M. Takita, M. Brink, J. M. Chow, and J. M. Gambetta, Hardware-efficient variational quantum eigensolver for small molecules and quantum magnets, *Nature* **549**, 242 (2017).
- [30] C. Hempel, C. Maier, J. Romero, J. McClean, T. Monz, H. Shen, P. Jurcevic, B. P. Lanyon, P. Love, R. Babbush, A. Aspuru-Guzik, R. Blatt, and C. F. Roos, Quantum Chemistry Calculations on a Trapped-Ion Quantum Simulator, *Phys. Rev. X* **8**, 031022 (2018).
- [31] J. Romero, R. Babbush, J. R. McClean, C. Hempel, P. J. Love, and A. Aspuru-Guzik, Strategies for quantum computing molecular energies using the unitary coupled cluster ansatz, *Quantum Science and Technology* **4**, 014008 (2018).
- [32] O. Higgott, D. Wang, and S. Brierley, Variational Quantum Computation of Excited States, arXiv preprint arXiv:1805.08138 (2018).
- [33] J. R. McClean, M. E. Kimchi-Schwartz, J. Carter, and W. A. de Jong, Hybrid quantum-classical hierarchy for mitigation of decoherence and determination of excited states, *Physical Review A* **95**, 042308 (2017).
- [34] J. I. Colless, V. V. Ramasesh, D. Dahlen, M. S. Blok, J. R. McClean, J. Carter, W. A. de Jong, and I. Siddiqi, Robust determination of molecular spectra on a quantum processor, arXiv preprint arXiv:1707.06408 (2017).
- [35] C. Kokail, C. Maier, R. van Bijnen, T. Brydges, M. K. Joshi, P. Jurcevic, C. A. Muschik, P. Silvi, R. Blatt, C. F. Roos, *et al.*, Self-verifying variational quantum simulation of lattice models, *Nature* **569**, 355 (2019).
- [36] K. Sharma, S. Khatri, M. Cerezo, and P. J. Coles, Noise resilience of variational quantum compiling, *New Journal of Physics* **22**, 043006 (2020).
- [37] M. Cerezo, K. Sharma, A. Arrasmith, and P. J. Coles, Variational Quantum State Eigensolver, arXiv preprint arXiv:2004.01372 (2020).
- [38] B. Koczor, S. Endo, T. Jones, Y. Matsuzaki, and S. C. Benjamin, Variational-State Quantum Metrology, *New J. Phys.* **22**, 083038 (2020).
- [39] B. Koczor and S. C. Benjamin, Quantum natural gradient generalised to non-unitary circuits, arXiv preprint arXiv:1912.08660 (2019).
- [40] B. Koczor and S. C. Benjamin, Quantum analytic descent, arXiv preprint arXiv:2008.13774 (2020).

[41] X. Yuan, S. Endo, Q. Zhao, Y. Li, and S. C. Benjamin, Theory of variational quantum simulation, *Quantum* **3**, 191 (2019).

[42] O. Crawford, B. van Straaten, D. Wang, T. Parks, E. Campbell, and S. Brierley, Efficient quantum measurement of Pauli operators, arXiv preprint arXiv:1908.06942 (2019).

[43] C. Hadfield, S. Bravyi, R. Raymond, and A. Mezzacapo, Measurements of Quantum Hamiltonians with Locally-Biased Classical Shadows, arXiv preprint arXiv:2006.15788 (2020).

[44] B. Koczor, To appear, (2021).

[45] A. Rényi, On measures of information and entropy, in *Proceedings of the 4th Berkeley symposium on mathematics, statistics and probability*, Vol. 1 (1961).

[46] R. Harper, W. Yu, and S. T. Flammia, Fast estimation of sparse quantum noise, arXiv preprint arXiv:2007.07901 (2020).

[47] B. van Straaten and B. Koczor, Measurement cost of metric-aware variational quantum algorithms, arXiv preprint arXiv:2005.05172 (2020).

[48] F. Roberts and B. Tesman, *Applied combinatorics* (CRC Press, 2009).

[49] B. E. Sagan, *The symmetric group: representations, combinatorial algorithms, and symmetric functions*, Vol. 203 (Springer Science & Business Media, 2013).

[50] A. K. Ekert, C. M. Alves, D. K. Oi, M. Horodecki, P. Horodecki, and L. C. Kwek, Direct estimations of linear and nonlinear functionals of a quantum state, *Phys. Rev. Lett.* **88**, 217901 (2002).

[51] J. Dénes, The representation of a permutation as the product of a minimal number of transpositions and its connection with the theory of graphs, *Publ. Math. Inst. Hungar. Acad. Sci* **4**, 63 (1959).

[52] Z. Cai, Multi-exponential error extrapolation and combining error mitigation techniques for nisq applications, arXiv preprint arXiv:2007.01265 (2020).

[53] M. Silva, E. Magesan, D. W. Kribs, and J. Emerson, Scalable protocol for identification of correctable codes, *Phys. Rev. A* **78**, 012347 (2008).

[54] E. Magesan, J. M. Gambetta, and J. Emerson, Characterizing quantum gates via randomized benchmarking, *Phys. Rev. A* **85**, 042311 (2012).

[55] Z. Cai and S. C. Benjamin, Constructing smaller pauli twirling sets for arbitrary error channels, *Sci. Rep.* **9**, 1 (2019).

[56] Z. Cai, X. Xu, and S. C. Benjamin, Mitigating coherent noise using Pauli conjugation, *npj Quantum Info.* **6**, 1 (2020).

[57] M. Keyl and R. F. Werner, Estimating the spectrum of a density operator, *Phys. Rev. A* **64**, 052311 (2001).

[58] I. Marvian and R. W. Spekkens, A generalization of Schur–Weyl duality with applications in quantum estimation, *Communications in Mathematical Physics* **331**, 431 (2014).

[59] J. Acharya, I. Issa, N. V. Shende, and A. B. Wagner, Estimating Quantum Entropy, *IEEE Journal on Selected Areas in Information Theory* **1**, 454 (2020).

[60] T. Tanaka, Y. Ota, M. Kanazawa, G. Kimura, H. Nakazato, and F. Nori, Determining eigenvalues of a density matrix with minimal information in a single experimental setting, *Phys. Rev. A* **89**, 012117 (2014).

[61] M. Christandl, A. W. Harrow, and G. Mitchison, Nonzero Kronecker coefficients and what they tell us about spectra, *Comm. Math. Phys.* **270**, 575 (2007).

[62] M. Christandl and G. Mitchison, The spectra of quantum states and the Kronecker coefficients of the symmetric group, *Communications in mathematical physics* **261**, 789 (2006).

[63] P. Horodecki, From limits of quantum operations to multicopy entanglement witnesses and state-spectrum estimation, *Phys. Rev. A* **68**, 052101 (2003).

[64] P. Horodecki, Measuring Quantum Entanglement without Prior State Reconstruction, *Phys. Rev. Lett.* **90**, 167901 (2003).

[65] P. Horodecki and A. Ekert, Method for Direct Detection of Quantum Entanglement, *Phys. Rev. Lett.* **89**, 127902 (2002).

[66] J. Fiurášek, M. Dušek, and R. Filip, Universal Measurement Apparatus Controlled by Quantum Software, *Phys. Rev. Lett.* **89**, 190401 (2002).

[67] M. Dušek and V. Bužek, Quantum-controlled measurement device for quantum-state discrimination, *Phys. Rev. A* **66**, 022112 (2002).

[68] R. Filip, Overlap and entanglement-witness measurements, *Phys. Rev. A* **65**, 062320 (2002).

[69] U. Chabaud, E. Diamanti, D. Markham, E. Kashefi, and A. Joux, Optimal quantum-programmable projective measurement with linear optics, *Phys. Rev. A* **98**, 062318 (2018).

[70] C. H. Bennett, G. Brassard, S. Popescu, B. Schumacher, J. A. Smolin, and W. K. Wootters, Purification of Noisy Entanglement and Faithful Teleportation via Noisy Channels, *Phys. Rev. Lett.* **76**, 722 (1996).

[71] N. Kalb, A. A. Reiserer, P. C. Humphreys, J. J. Bakermans, S. J. Kamerling, N. H. Nickerson, S. C. Benjamin, D. J. Twitchen, M. Markham, and R. Hanson, Entanglement distillation between solid-state quantum network nodes, *Science* **356**, 928 (2017).

[72] D. Deutsch, A. Ekert, R. Jozsa, C. Macchiavello, S. Popescu, and A. Sanpera, Quantum privacy amplification and the security of quantum cryptography over noisy channels, *Phys. Rev. Lett.* **77**, 2818 (1996).

[73] T. Jones and S. C. Benjamin, QuESTlink–Mathematica embiggened by a hardware-optimised quantum emulator, *Quantum Science and Technology* (2020).

Supplementary Materials

Exponential Error Suppression for Near-Term Quantum Devices

Appendix A: Derangement measurements and suppressing errors

In this section we prove that the derangement circuit in Fig. 1 can be used to estimate expectation values. We then prove upper bounds on approximation errors with or without using Rényi entropies of quantum states. We finally prove sample complexities of our ESD approach.

Definition 1. *We define the set \mathfrak{D}_n of derangement operators that permute $n \geq 2$ quantum registers via their unitary representation as*

$$\text{every } D_n \in \mathfrak{D}_n, \text{ is such that } D_n |\psi_1, \psi_2, \dots, \psi_n\rangle = |\psi_{s(1)}, \psi_{s(2)}, \dots, \psi_{s(n)}\rangle.$$

Here all $s \in S_n$ are permutations of the index set $\{1, 2, \dots, n\}$ with no fixed point, i.e., s are derangements [48, 49]. Here S_n denotes the symmetric group. For $n \geq 4$ we also demand that s are n -cycles (standard cyclic permutations of maximal length [49]), which are a subset of derangements. The number of unique (n -cycle) derangement operators is given as $|\mathfrak{D}_n| = (n-1)!$. Due to seminal results of Dénes, s can be decomposed into $n-1$ transpositions [51] and therefore D_n decomposes into $n-1$ pair-wise SWAP operators of the quantum registers. One can therefore construct minimal SWAP circuits by (bijectively) mapping the corresponding permutations performed by $D_n \in \mathfrak{D}_n$ to graph trees.

Theorem 1. *We consider n identical copies of the same quantum register ρ in a separable state as $\rho^{\otimes n}$. Methods A and B, as illustrated in Fig. 1, result in the probability of measuring the ancilla in the 0 state as*

$$\text{Method A/B: } \text{prob}_0 = \frac{1}{2} + \frac{1}{2} \text{Tr}[\rho^n \sigma]. \quad (\text{A1})$$

Here σ is a unitary (Hermitian) observable (or otherwise the real part of a unitary operator is estimated).

Proof. We start by recapitulating that any density operator ρ admits the following spectral decomposition (note that here we use a different notation than what in the main text)

$$\rho = \sum_{k=1}^d p_k |\psi_k\rangle\langle\psi_k|, \quad \text{thus} \quad \rho^{\otimes n} = \sum_{k_1, k_2, \dots, k_n=1}^{2^N} p_{k_1} p_{k_2} \cdots p_{k_n} |\psi_{k_1}, \psi_{k_2}, \dots, \psi_{k_n}\rangle\langle\psi_{k_1}, \psi_{k_2}, \dots, \psi_{k_n}|, \quad (\text{A2})$$

where the second equation is the spectral decomposition of n copies of the same state.

Recall that the action of any unitary circuit U on a density matrix $U\rho U^\dagger$ represents a probabilistic mixture of its transformed eigenvectors $U|\psi_k\rangle$ that occur with probabilities p_k . Similarly the action of a unitary circuit on the composite state $\rho^{\otimes n}$ can be written as a probabilistic mixture of the pure-states $U|\psi_{k_1}, \psi_{k_2}, \dots, \psi_{k_n}\rangle$ that occur with probabilities as products $p_{k_1} p_{k_2} \cdots p_{k_n}$.

Let us now derive the action of the unitary circuit in Fig. 1 on the composite quantum system $\rho^{\otimes n}$. Our proof works with any derangement operator D_n from Definition 1 but here we only need to consider one example: we consider a cyclic shift (as originally proposed in [50]) of the registers via its explicit action on pure states as

$$D_n |\psi_1, \psi_2, \dots, \psi_n\rangle = |\psi_n, \psi_1, \dots, \psi_{n-1}\rangle.$$

Our controlled derangement operator acts on the pure state $|0, \psi_{k_1}, \psi_{k_2}, \dots, \psi_{k_n}\rangle$ that occurs with a probability $p_{k_1} p_{k_2} \cdots p_{k_n}$, and we denote as 0 the state of the additional ancilla qubit. Applying the sequence of gates from Fig. 1

yields the following transformations of the pure states.

$$\begin{aligned}
& |0, \psi_{k_1}, \psi_{k_2}, \dots, \psi_{k_n}\rangle \\
& \quad \downarrow H \\
& (|1, \psi_{k_1}, \psi_{k_2}, \dots, \psi_{k_n}\rangle + |0, \psi_{k_1}, \psi_{k_2}, \dots, \psi_{k_n}\rangle) / \sqrt{2} \\
& \quad \downarrow \text{controlled } D_n \\
& (|1, \psi_{k_n}, \psi_{k_1}, \dots, \psi_{k_{n-1}}\rangle + |0, \psi_{k_1}, \psi_{k_2}, \dots, \psi_{k_n}\rangle) / \sqrt{2} \\
& \quad \downarrow \text{controlled } \sigma \\
& (|1, \sigma\psi_{k_n}, \psi_{k_1}, \dots, \psi_{k_{n-1}}\rangle + |0, \psi_{k_1}, \psi_{k_2}, \dots, \psi_{k_n}\rangle) / \sqrt{2} \\
& \quad \downarrow H \\
& (|0, \sigma\psi_{k_n}, \psi_{k_1}, \dots, \psi_{k_{n-1}}\rangle + |0, \psi_{k_1}, \psi_{k_2}, \dots, \psi_{k_n}\rangle) / 2 + \dots
\end{aligned}$$

It is now straightforward to show that the probability of measuring the ancilla qubit in state 0 is

$$\text{prob}_0 = \frac{1}{2} + \frac{1}{2} \sum_{k_1, k_2, \dots, k_n=1}^{2^N} p_{k_1} p_{k_2} \cdots p_{k_n} \langle \psi_{k_1}, \psi_{k_2}, \dots, \psi_{k_n} | \sigma \psi_{k_n}, \psi_{k_1}, \dots, \psi_{k_{n-1}} \rangle, \quad (\text{A3})$$

where we can simplify the inner products as

$$\langle \psi_{k_1}, \psi_{k_2}, \dots, \psi_{k_n} | \sigma \psi_{k_n}, \psi_{k_1}, \dots, \psi_{k_{n-1}} \rangle = \langle \psi_{k_1} | \sigma \psi_{k_n} \rangle \langle \psi_{k_2} | \psi_{k_1} \rangle \cdots \langle \psi_{k_n} | \psi_{k_{n-1}} \rangle = \langle \psi_{k_1} | \sigma \psi_{k_n} \rangle \delta_{k_2 k_1} \cdots \delta_{k_n k_{n-1}}, \quad (\text{A4})$$

and we have used the orthogonality of the eigenstates $|\psi_k\rangle$ and δ_{ab} is the Kroenecker delta symbol. At this point we remark that our proof works with any derangement operator from Definition 1 since these will conserve the above orthonormality relation. We remark here that the corresponding permutations can be mapped to graph trees, which represent the pairs of indexes δ_{ab} in the Kroenecker delta symbols in the above equation.

Substituting the above results back we obtain the expression for the ancilla probability by using that only terms with coinciding indexes contribute to the sum via $k_1 = k_2 = \dots = k_n$

$$\text{prob}_0 = \frac{1}{2} + \frac{1}{2} \sum_{k=1}^{2^N} p_k^n \langle \psi_k | \sigma | \psi_k \rangle = \frac{1}{2} + \frac{1}{2} \text{Tr}[\rho^n \sigma]. \quad (\text{A5})$$

□

Example 1. Using our definition of experimental quantum states from Eq. (1), our circuit in Fig. 1 can estimate the expectation value

$$\text{Tr}[\rho^n \sigma] = \lambda^n \langle \psi | \sigma | \psi \rangle + (1 - \lambda)^n \sum_{k=2}^{2^N} p_k^n \langle \psi_k | \sigma | \psi_k \rangle.$$

It is clear that the error probabilities p_k are suppressed exponentially via p_k^n , but the dominant term gets slightly attenuated too via λ^n . For example, let us assume that our dominant eigenvalue is $\lambda = 0.8$ and we have a high-entropy error in a subspace spanned by 100 eigenvectors via the uniform distribution $p_k = (1 - \lambda)/100$ when $k \leq 101$ and $p_k = 0$ when $k > 101$. We then obtain the estimate

$$\text{Tr}[\rho^n \sigma] = 0.8^n \langle \psi | \sigma | \psi \rangle + \sum_{k=2}^{101} (2 \times 10^{-3})^n \langle \psi_k | \sigma | \psi_k \rangle.$$

Since $|\langle \psi_k | \sigma | \psi_k \rangle| \leq 1$, we can upper bound the errors in, e.g., for $n = 3$ as $\text{Tr}[\rho^n \sigma] = 0.512 \langle \psi | \sigma | \psi \rangle + E$ with $|E| \leq 8 \times 10^{-7}$. Hence our error contribution is at least 640000-times smaller than the desired expectation value. This high degree of error suppression is due to the large $n = 3$ Rényi entropy of the error probabilities p_k as

$$H_3(p) = -\frac{1}{2} \ln \left[\sum_{k=2}^{2^N} p_k^n \right] = -\frac{1}{2} \ln \left[\sum_{k=2}^{101} (10^{-2})^3 \right] \approx -\frac{1}{2} \ln [10^{-4}] \approx 4.6.$$

We will show in Theorem 2 and in Lemma 1 that the efficiency of the error suppression depends exponentially on this Rényi entropy.

Indeed, in order to obtain an accurate estimate of $\langle \psi | \sigma | \psi \rangle$ we need to have a good knowledge of the largest eigenvalue of the density matrix λ that divides $\langle \psi | \sigma | \psi \rangle$. We assume in Method B in Theorem 2 that this eigenvalue is known precisely. However, in Method A we just replace our observable σ with the identity in Fig. 1 and we directly approximate the n^{th} power of the dominant eigenvalue λ as

$$\text{Tr}[\rho^n] = 0.8^n + \sum_{k=2}^{101} (2 \times 10^{-3})^n,$$

for $n = 3$ we obtain the result as $0.8^3 + 8 \times 10^{-7} = 0.512001$, which is a very good estimate of $0.8^3 = 0.512$ as the error is 640000-times smaller than the ideal value.

Example 2. We consider now the worst-case scenario of 0-entropy error distributions. For example, let us consider the state $\rho = \lambda|\psi\rangle\langle\psi| + (1 - \lambda)|\psi_{err}\rangle\langle\psi_{err}|$ which is a mixture of the ideal state $|\psi\rangle$ that occurs with a probability λ and an erroneous state $|\psi_{err}\rangle$ which occurs with a probability $(1 - \lambda)$. The error probability distribution from Eq. (1) is obtained as $p_2 = 1$ and $p_k = 0$ for $k > 2$. It follows that the error distribution has a 0 entropy and our approach completely breaks down when $\lambda \leq 1/2$ since the dominant eigenvector then becomes $|\psi_{err}\rangle$. We can show that the errors in the expectation value are still exponentially suppressed, but much less efficiently than before in Example 1. Let us set $\lambda = 0.8$ and

$$\text{Tr}[\rho^n \sigma] = 0.8^n \langle \psi | \sigma | \psi \rangle + 0.2^n \langle \psi_{err} | \sigma | \psi_{err} \rangle.$$

For $n = 3$ we obtain $\text{Tr}[\rho^3 \sigma] = 0.512 \langle \psi | \sigma | \psi \rangle + 0.008 \langle \psi_{err} | \sigma | \psi_{err} \rangle$, and therefore the error is suppressed by a factor of 64. This is significantly lower than the factor of 640000 suppression from Example 1 which assumed a high-entropy error distribution.

Appendix B: Exponentially decreasing upper bounds on approximation errors

Theorem 2. *We use Methods A/B from Fig. 1 to estimate the probability $\text{prob}_0 = \frac{1}{2} + \frac{1}{2}\text{Tr}[\rho^n\sigma]$ of the ancilla qubit. In Method A we use the same technique via $\sigma = \text{Id}$ to estimate the probability $\text{prob}'_0 = \frac{1}{2} + \frac{1}{2}\text{Tr}[\rho^n]$ and our Method A yields the approximation*

$$\text{Method A: } \frac{2\text{prob}_0 - 1}{2\text{prob}'_0 - 1} = \frac{\text{Tr}[\rho^n\sigma]}{\text{Tr}[\rho^n]} = \langle\psi|\sigma|\psi\rangle + \mathcal{E}_A.$$

In Method B we assume that the largest eigenvalue λ of the state ρ is known and therefore we have the approximation

$$\text{Method B: } (2\text{prob}_0 - 1)/\lambda^n = \text{Tr}[\rho^n\sigma]/\lambda^n = \langle\psi|\sigma|\psi\rangle + \mathcal{E}_B.$$

The approximation errors are bounded via $|\mathcal{E}_A| \leq \frac{2Q_n}{1+Q_n}$ and $|\mathcal{E}_B| \leq Q_n$, and we prove in Lemma 1 that the bounding sequence $Q_n = (\lambda^{-1} - 1)^n \|\underline{p}\|_n^n$ generally decays exponentially when we increase n or when we increase the Rényi entropy of the probability vector \underline{p} .

Proof. Let us recapitulate the explicit form of the density matrix from Eq. (1) as

$$\rho = \lambda|\psi\rangle\langle\psi| + (1 - \lambda) \sum_{k=2}^{2^N} p_k |\psi_k\rangle\langle\psi_k|. \quad (\text{B1})$$

We can evaluate the expressions for the trace operation as

$$\text{Tr}[\rho^n\sigma] = \lambda^n \langle\psi|\sigma|\psi\rangle + (1 - \lambda)^n \sum_{k=2}^{2^N} p_k^n \langle\psi_k|\sigma|\psi_k\rangle, \quad \text{and} \quad \left| \sum_{k=2}^{2^N} p_k^n \langle\psi_k|\sigma|\psi_k\rangle \right| \leq \sum_{k=2}^{2^N} p_k^n = \|\underline{p}\|_n^n,$$

where we have used that $\langle\psi_k|\sigma|\psi_k\rangle \leq 1$ due to unitarity of σ and $\|\underline{p}\|_n$ is the n -norm of the probability vector \underline{p} .

Method B: Here our aim is to estimate $\text{Tr}[\rho^n\sigma]$ and λ^n is known exactly. The error term can be calculated via

$$|\mathcal{E}_B| = \left| \frac{\text{Tr}[\rho^n\sigma]}{\lambda^n} - \langle\psi|\sigma|\psi\rangle \right| = \frac{(1 - \lambda)^n}{\lambda^n} \left| \sum_{k=2}^{2^N} p_k^n \langle\psi_k|\sigma|\psi_k\rangle \right| \leq \frac{(1 - \lambda)^n}{\lambda^n} \|\underline{p}\|_n^n =: Q_n, \quad (\text{B2})$$

and here we have defined the suppression factor Q .

Method A: In this case we estimate $\text{Tr}[\rho^n\sigma]$ and $\text{Tr}[\rho^n]$, and we now calculate the error term using that $\text{Tr}[\rho^n] = \lambda^n + (1 - \lambda)^n \sum_k p_k^n = \lambda^n + (1 - \lambda)^n \|\underline{p}\|_n^n$. Indeed, we obtain

$$|\mathcal{E}_A| = \left| \frac{\text{Tr}[\rho^n\sigma]}{\text{Tr}[\rho^n]} - \langle\psi|\sigma|\psi\rangle \right| = \left| \frac{\langle\psi|\sigma|\psi\rangle + \lambda^{-n}(1 - \lambda)^n \sum_{k=2}^{2^N} p_k^n \langle\psi_k|\sigma|\psi_k\rangle}{1 + \lambda^{-n}(1 - \lambda)^n \|\underline{p}\|_n^n} - \langle\psi|\sigma|\psi\rangle \right| = \left| \frac{\langle\psi|\sigma|\psi\rangle + Z}{1 + Q_n} - \langle\psi|\sigma|\psi\rangle \right|, \quad (\text{B3})$$

where we have used the notation $Z = \lambda^{-n}(1 - \lambda)^n \sum_{k=2}^{2^N} p_k^n \langle\psi_k|\sigma|\psi_k\rangle$ for simplicity. It follows that the error term is bounded via

$$|\mathcal{E}_A| = \left| \frac{\langle\psi|\sigma|\psi\rangle + Z}{1 + Q_n} - \langle\psi|\sigma|\psi\rangle \right| = \left| \frac{Z - Q_n \langle\psi|\sigma|\psi\rangle}{1 + Q_n} \right|. \quad (\text{B4})$$

Let us now upper bound this expression as

$$(1 + Q_n)^{-1} |Z - Q_n \langle\psi|\sigma|\psi\rangle| \leq (1 + Q_n)^{-1} [|Z| + Q_n |\langle\psi|\sigma|\psi\rangle|], \quad (\text{B5})$$

where we have used the triangle inequality as $|a - b| \leq |a| + |b|$. We can now use from before that $|Z| \leq Q_n$, which results in the error term

$$|\mathcal{E}_A| \leq \frac{Q_n + Q_n |\langle\psi|\sigma|\psi\rangle|}{1 + Q_n} = \frac{Q_n}{1 + Q_n} (1 + |\langle\psi|\sigma|\psi\rangle|) \leq \frac{2Q_n}{1 + Q_n}. \quad (\text{B6})$$

This concludes our proof. \square

Lemma 1. *The sequence Q_n in our upper bounds in Theorem 2 decreases exponentially for a fixed n when we increase the Rényi entropy $H_n(\underline{p})$ of the error probability vector \underline{p} from Eq. (1) as $Q_n = (\lambda^{-1}-1)^n \exp[-(n-1)H_n(\underline{p})]$. Furthermore, the sequence generally decays exponentially via $Q_n \leq (p_{\max})^{-1}Q^n$ where we define the suppression factor $Q := (\lambda^{-1}-1)p_{\max} < 1$ and p_{\max} is the largest error probability from Eq. (1).*

Proof. The first part of the proof straightforwardly follows by substituting the expression for the Rényi entropy [45]

$$H_n(\underline{p}) = \frac{1}{1-n} \ln \left[\sum_{k=2}^{2^n} p_k^n \right] = \frac{n}{1-n} \ln \|\underline{p}\|_n, \quad (\text{B7})$$

into the expression for Q as

$$Q_n = [(\lambda^{-1}-1)\|\underline{p}\|_n]^n = (\lambda^{-1}-1)^n \exp[-\frac{n-1}{n} H_n(\underline{p})]^n = (\lambda^{-1}-1)^n \exp[-(n-1)H_n(\underline{p})].$$

This concludes the first part of our proof.

Let us now prove that the sequence Q_n decreases in exponential order when we increase n . Using the well-known series of inequalities satisfied by the Rényi entropies as $H_\infty(\underline{p}) \leq H_n(\underline{p}) \leq H_{n-1}(\underline{p}) \leq \dots \leq H_1(\underline{p})$, we obtain the general bound $-\ln p_{\max} \leq H_n(\underline{p})$ for all n , and we define the largest error probability $p_{\max} := \max_k p_k$. It follows that

$$Q_n \leq (\lambda^{-1}-1)^n (p_{\max})^{n-1} = (p_{\max})^{-1} [(\lambda^{-1}-1)p_{\max}]^n =: (p_{\max})^{-1} Q^n.$$

The upper bound $Q < 1$ holds due to our condition below Eq. (1) as $(\lambda-1)p_k < \lambda$ for every probability $k = \{2, 3, \dots, 2^N\}$. It follows that $p_{\max} < (\lambda^{-1}-1)^{-1}$ and therefore $Q = (\lambda^{-1}-1)p_{\max} < 1$. \square

Lemma 2. *Determining the expectation value $\langle \psi | \sigma | \psi \rangle$ from Theorem 2 to a fixed precision \mathcal{E} requires $n = \frac{\ln \mathcal{E}^{-1} + \ln [2(p_{\max})^{-1}]}{\ln Q^{-1}}$ copies of the quantum state ρ (one needs to apply the ceiling function to round this up to the nearest integer). Here $Q < 1$ is the suppression factor from Theorem 2 and from Lemma 1.*

Reducing shot noise to the desired precision \mathcal{E} requires the following number of samples. In Method A one needs to assign $N_{s,1}$ samples to determine prob_0 and $N_{s,2}$ samples to determine prob'_0 as

$$\text{Method A:} \quad N_{s,1} = \mathcal{O}[\mathcal{E}^{-2(1+f)}] = \text{poly}(\mathcal{E}^{-1}) \quad \text{and} \quad N_{s,2} = \mathcal{O}[\mathcal{E}^{-2(1+2f)}] = \text{poly}(\mathcal{E}^{-1}). \quad (\text{B8})$$

The overall number of measurements required is $N_s = N_{s,1} + N_{s,2} = \mathcal{O}[\mathcal{E}^{-2(1+2f)}]$. In Method B one only needs to determine prob_0 since λ^n is known. The number of samples scales as

$$\text{Method B:} \quad N_s = \mathcal{O}[\mathcal{E}^{-2(1+f)}] = \text{poly}(\mathcal{E}^{-1}). \quad (\text{B9})$$

Indeed, in both cases the measurement cost grows polynomially with the inverse precision \mathcal{E}^{-1} and its polynomial order is determined by $f := \frac{\ln(\lambda^{-1})}{\ln(Q^{-1})}$. The standard shot-noise limit \mathcal{E}^{-2} is only slightly modified by f in case of good quality quantum states or in case of high-entropy probabilities.

Proof. Let us first compute the upper bound on the number of copies n required to achieve a fixed precision $\mathcal{E} \ll 1$. We use the upper bounds from Theorem 2 as $|\mathcal{E}_A| \leq \mathcal{E} = \frac{2Q_n}{1+Q_n} \approx 2Q_n$ and $|\mathcal{E}_B| \leq \mathcal{E} = Q_n$. It is clear that the precision of Method A differs by a factor of 2 for $\mathcal{E} \ll 1$, and we will use this expression for both methods for simplicity. Let us use the exponentially decreasing upper bounds on Q_n from Lemma 1 and write $|\mathcal{E}_A| \leq 2(p_{\max})^{-1}Q^n$, and $|\mathcal{E}_B| \leq 2(p_{\max})^{-1}Q^n$, where we have defined the suppression factor as $Q := (\lambda^{-1}-1)p_{\max} < 1$. It is straightforward to express n as

$$n = \frac{\ln \mathcal{E}^{-1} + \ln [2(p_{\max})^{-1}]}{\ln Q^{-1}}. \quad (\text{B10})$$

Remark: Let us further expand the above equation by using our expression from Lemma 1 as $Q_n = (\lambda^{-1}-1)^n \exp[-(n-1)H_n(\underline{p})]$, which results in

$$-\ln(\mathcal{E}^{-1}) = \ln \mathcal{E} = \ln 2Q_n = \ln(2) + n \ln[(\lambda^{-1}-1)] - (n-1)H_n(\underline{p}) = \ln(2) + H_n(\underline{p}) + n\{\ln[(\lambda^{-1}-1)] - H_n(\underline{p})\}.$$

We can express n as

$$n = \frac{\ln(\mathcal{E}^{-1}) + H_n(\underline{p}) + \ln(2)}{H_n(\underline{p}) - \ln[(\lambda^{-1}-1)]} = \mathcal{O}(\ln(\mathcal{E}^{-1})).$$

We remark that the denominator is positive due to the bound on Rényi entropies from Lemma 1 as $\ln[(\lambda^{-1}-1)] < H_n(\underline{p})$. One should actually use the ceil function to round up the right-hand expression to the nearest integer. Note that the above expression implicitly depends on n via the Rényi entropy $H_n(\underline{p})$, but one could always use the series of inequalities $0 \leq H_n(\underline{p}) \leq H_{n-1}(\underline{p}) \leq \dots H_2(\underline{p}) \leq H_1(\underline{p})$ to bound the value of n . It is straightforward to show now that in the limiting scenarios $H_2(\underline{p}) \gg 1$ or $\lambda \approx 1$ we recover $n \rightarrow 1$ (via the ceil function). Let us now express the scaling with respect to shot noise.

Method B: We estimate the probability prob_0 from Theorem 2 and we exactly know λ^n . Our precision \mathcal{E} is determined by the variance of our estimator which can be obtained as

$$\mathcal{E}^2 = \text{Var}[\langle \psi | \sigma | \psi \rangle] = \text{Var}\left[\frac{2\text{prob}_0 - 1}{\lambda^n}\right] = \frac{4\text{Var}[\text{prob}_0]}{\lambda^{2n}} = \frac{4\text{prob}_0(1 - \text{prob}_0)}{N_s \lambda^{2n}}, \quad (\text{B11})$$

where we have used that the variance of the binomial distribution is $\text{prob}_0(1 - \text{prob}_0)/N_s$ and N_s is the number of samples. We can explicitly express the number of shots N_s required to reach a fixed precision \mathcal{E} as

$$N_s = \frac{4\text{prob}_0(1 - \text{prob}_0)}{\mathcal{E}^2 \lambda^{2n}}, \quad (\text{B12})$$

Let us now simplify λ^{2n} by expressing the dependence of n on the precision above \mathcal{E} as

$$\ln[\lambda^{2n}] = 2n \ln[\lambda] = 2 \ln[\lambda] \frac{\ln \mathcal{E}^{-1} + \ln[2(p_{\max})^{-1}]}{\ln Q^{-1}} = \ln \mathcal{E}^{-1} \frac{2 \ln[\lambda]}{\ln Q^{-1}} + \frac{\ln[\lambda] \ln[4(p_{\max})^{-2}]}{\ln Q^{-1}},$$

and it follows that

$$\lambda^{2n} = \exp[\ln \mathcal{E}^{-1} \frac{2 \ln[\lambda]}{\ln Q^{-1}} + \frac{\ln[\lambda] \ln[4(p_{\max})^{-2}]}{\ln Q^{-1}}] = \mathcal{E}^{\frac{2 \ln[\lambda^{-1}]}{\ln Q^{-1}}} \exp[\frac{\ln[\lambda] \ln[4(p_{\max})^{-2}]}{\ln Q^{-1}}]. \quad (\text{B13})$$

We can finally express the number of samples explicitly as

$$N_s = 4\text{prob}_0(1 - \text{prob}_0) \mathcal{E}^{-2[1 + \frac{\ln(\lambda^{-1})}{\ln(Q^{-1})}]} \exp[\frac{\ln(\lambda^{-1}) \ln[4(p_{\max})^{-2}]}{\ln(Q^{-1})}] = \mathcal{O}[\mathcal{E}^{-2(1+f)}] \quad (\text{B14})$$

Here we used that $4 \exp[\frac{\ln(\lambda^{-1}) \ln[4(p_{\max})^{-2}]}{\ln(Q^{-1})}]$ is a constant multiplication factor and $0 \leq \text{prob}_0 \leq 1$ and we have introduced $f := \frac{\ln(\lambda^{-1})}{\ln(Q^{-1})}$. Indeed, we obtain the expected limits due to $\lim_{\lambda \rightarrow 1} f = 0$ and $\lim_{Q \rightarrow 0} f = 0$. We can upper bound f by using $Q \leq (\lambda^{-1}-1)\sqrt{p_{\max}}$ for $n \geq 2$ and obtain $f \leq \frac{\ln(\lambda^{-1})}{-\ln[(\lambda^{-1}-1)\sqrt{p_{\max}}]}$.

In general when $\lambda > 1/2$ we can use the expression $Q \leq (\lambda^{-1}-1)$ from Theorem 2 as $f \leq \frac{\ln(\lambda^{-1})}{\ln[(\lambda^{-1}-1)-1]}$ which is only saturated by 0-entropy distributions. For example when $\lambda = 0.6$ then we obtain $f \leq 1.26$, and this value can be smaller depending on the entropy of the probability distribution. Interestingly, for sufficiently good quality states as $\lambda \geq 0.9$, the polynomial overhead introduced is very small via $f \leq 0.16$.

Method A: In this case we estimate both prob_0 and prob'_0 . The variance of our estimator can be specified as

$$\mathcal{E}^2 = \text{Var}[\langle \psi | \sigma | \psi \rangle] = \text{Var}\left[\frac{2\text{prob}_0 - 1}{2\text{prob}'_0 - 1}\right] = \text{Var}[\text{prob}_0] \frac{4}{(2\text{prob}'_0 - 1)^2} + \text{Var}[\text{prob}'_0] \frac{4(2\text{prob}_0 - 1)^2}{(2\text{prob}'_0 - 1)^4}.$$

Let us now use that $2\text{prob}'_0 - 1 \approx \lambda^n$ and simplify the above expression as

$$\mathcal{E}^2 = \text{Var}[\langle \psi | \sigma | \psi \rangle] \approx \text{Var}\left[\frac{2\text{prob}_0 - 1}{2\text{prob}'_0 - 1}\right] = \text{Var}[\text{prob}_0] \frac{4}{\lambda^{2n}} + \text{Var}[\text{prob}'_0] \frac{4(2\text{prob}_0 - 1)^2}{\lambda^{4n}}.$$

We can again substitute the variance of binomial distributions as $\text{Var}[\text{prob}_0] = \text{prob}_0(1 - \text{prob}_0)/N_{s,1}$ and $\text{Var}[\text{prob}'_0] = \text{prob}'_0(1 - \text{prob}'_0)/N_{s,2}$. The measurement cost of determining both components to a precision $\mathcal{E}^2/2$ follows as

$$N_{s,1} = \frac{8\text{prob}_0(1 - \text{prob}_0)}{\mathcal{E}^2 \lambda^{2n}} \quad \text{and} \quad N_{s,2} = \frac{8\text{prob}'_0(1 - \text{prob}'_0)(2\text{prob}_0 - 1)^2}{\mathcal{E}^2 \lambda^{4n}}$$

We can now use our previous expression from Eq. (B13) for determining λ^{2n} and λ^{4n} , which finally yields our formula for the measurement costs as

$$N_{s,1} = \mathcal{O}[\mathcal{E}^{-2(1+f)}] \quad \text{and} \quad N_{s,2} = \mathcal{O}[\mathcal{E}^{-2(1+2f)}]. \quad (\text{B15})$$

Total number of measurements required to determine the result is indeed $N_{s,1} + N_{s,2}$, and recall that $f = \frac{\ln(\lambda^{-1})}{\ln(Q^{-1})}$. \square

Appendix C: Effect of violating assumptions

Let us now analyse how non-identical copies of ρ affect the performance of our approach.

Lemma 3. *When the states are not perfectly identical via $\rho = \bigotimes_{\mu=1}^n \rho_\mu$ with $\rho_1 \neq \rho_2 \dots \neq \rho_n$, but their largest eigenvector is identical then our main result from Theorem 2 still holds and we still obtain exponentially decreasing error bounds as*

$$\begin{aligned} \text{Method A: } \frac{2\text{prob}_0 - 1}{2\text{prob}'_0 - 1} &= \langle \psi | \sigma | \psi \rangle + \mathcal{O}([\lambda_{\min}^{-1} - 1]^n), \\ \text{Method B: } \frac{2\text{prob}_0 - 1}{\prod_{\mu=1}^n \lambda_\mu} &= \langle \psi | \sigma | \psi \rangle + \mathcal{O}([\lambda_{\min}^{-1} - 1]^n). \end{aligned}$$

For Method B we assume that the dominant eigenvalues $\lambda_1, \lambda_2, \dots, \lambda_n$ are known. The error depends on the smallest of these dominant eigenvalues, which we denote as λ_{\min} . In the special case when all ρ_μ commute (i.e., same eigenvectors, but different eigenvalues) our error bounds \mathcal{E}_A and \mathcal{E}_B from Theorem 2 approximately holds via an effective suppression factor Q_n^{eff} , and we can expect an error suppression very similar to Theorem 2.

Proof. **Case 1:** Let us build up components of our proof by first considering the special case when all ρ_k commute with each other. In other words the states staisfy the spectral decomposition

$$\rho_\mu = \lambda_\mu |\psi\rangle\langle\psi| + (1 - \lambda_\mu) \sum_{k=2}^d p_{k,\mu} |\psi_k\rangle\langle\psi_k|,$$

and they all share the same eigenvectors while their eigenvalues can be different. It follows that the orthogonality relations in the proof of Theorem 1 in Eq. (A4) still hold and the final result can be written explicitly as

$$\text{prob}_0 = \frac{1}{2} + \frac{1}{2} \langle \psi | \sigma | \psi \rangle \prod_{\mu=1}^n \lambda_\mu + \sum_{k=2}^d \langle \psi_k | \sigma | \psi_k \rangle \prod_{\mu=1}^n p_{k,\mu} (1 - \lambda_\mu). \quad (\text{C1})$$

We can upper bound the error term in the above expression as

$$|\sum_{k=2}^d \langle \psi_k | \sigma | \psi_k \rangle \prod_{\mu=1}^n p_{k,\mu} (1 - \lambda_\mu)| \leq (1 - \lambda_{\min})^n \sum_{k=2}^d (p_{k,\max})^n, \quad (\text{C2})$$

where we have denoted the largest component as $\lambda_{\min} = \min_\mu \mu \lambda_\mu$ and $p_{k,\max} = \max_\mu p_{k,\mu}$ and we have also used that $|\langle \psi_k | \sigma | \psi_k \rangle| \leq 1$.

We can also upper bound the product $\prod_{\mu=1}^n \lambda_\mu \geq \lambda_{\min}^n$ and derive the error of our Method A in Theorem 2 which results in

$$\frac{2\text{prob}_0 - 1}{2\text{prob}'_0 - 1} = \langle \psi | \sigma | \psi \rangle + \mathcal{E}_A, \quad \text{with} \quad |\mathcal{E}_A| \leq \frac{2Q_n^{\text{eff}}}{1 + Q_n^{\text{eff}}}$$

which we write in terms of an effective quality factor $Q_n^{\text{eff}} = (\lambda_{\min}^{-1} - 1)^n \|p_{\max}\|_n^n$.

We can similarly derive the errors of our Method B in Theorem 2 in case when the eigenvalues $\lambda_1, \lambda_2, \dots, \lambda_n$ are known. This results in

$$\frac{2\text{prob}_0 - 1}{\prod_{\mu=1}^n \lambda_\mu} = \langle \psi | \sigma | \psi \rangle + \mathcal{E}_B, \quad \text{with} \quad |\mathcal{E}_B| \leq Q_n^{\text{eff}},$$

where we have again used our effective suppression factor $Q_n^{\text{eff}} = (\lambda_{\min}^{-1} - 1)^n \|p_{\max}\|_n^n$. We note that here p_{\max} is no longer a proper probability vector since $\sum_{k=2}^d p_{k,\max} \geq 1$ and therefore we cannot guarantee in general that $Q_{\text{eff}} < 1$. Nevertheless, one expect a very similar exponential decay of the error as in Theorem 2 and in Lemma 1 for high-entropy probability distributions and for $n > 1$.

Case 2: We now consider the most general case when ρ_μ are arbitrary except that their dominant eigenvector is exactly $|\psi\rangle$. The states therefore admit the following spectral decompositon

$$\rho_\mu = \lambda_\mu |\psi\rangle\langle\psi| + (1 - \lambda_\mu) \sum_{k=2}^d p_{k,\mu} |\psi_{k,\mu}\rangle\langle\psi_{k,\mu}|,$$

It follows from the above definition that the dominant eigenvector $|\psi\rangle$ is orthogonal to every error contribution in every eigenstate as $\langle\psi|\psi_{k_\mu}\rangle = 0$ for every $k = \{1, \dots, 2^N\}$ and for every $\mu = \{1, \dots, n\}$. Modifying accordingly the orthogonality relation in the proof of Theorem 1 in Eq. (A4) allows us to compute the leading term as expected, but every other non-zero term is multiplied with the prefactor $\prod_{\mu=1}^n (1 - \lambda_\mu)$ which leads to the following error term

$$\text{prob}_0 = \frac{1}{2} + \frac{1}{2} \langle\psi|\sigma|\psi\rangle \prod_{\mu=1}^n \lambda_\mu + \mathcal{O}\left[\prod_{\mu=1}^n (1 - \lambda_\mu)\right]. \quad (\text{C3})$$

As shown previously, this allows us to compute the error of our Method A and Method B in Theorem 2 as

$$\frac{2\text{prob}_0 - 1}{2\text{prob}'_0 - 1} = \langle\psi|\sigma|\psi\rangle + \mathcal{O}([\lambda_{\min}^{-1} - 1]^n), \quad \text{and} \quad \frac{2\text{prob}_0 - 1}{\prod_{\mu=1}^n \lambda_\mu} = \langle\psi|\sigma|\psi\rangle + \mathcal{O}([\lambda_{\min}^{-1} - 1]^n),$$

in general for $\lambda_{\min} > 1/2$. \square

1. Coherent mismatch in incoherent error channels

As we discussed in the main text our approach cannot address coherent errors, i.e., when the dominant eigenvector of the density matrix is $\sqrt{1-c}|\psi_{id}\rangle + \sqrt{c}|\psi_{err}\rangle$, where ψ_{id} is the ideal computation state and ψ_{err} is some error. This is expected to happen when systematic errors, such as miscalibrated rotation angles, are present but it is straightforward to show that even a completely incoherent error channel (random unitary events) can introduce a slight mismatch in the eigenvectors.

We show this by considering a quite general noise channel as

$$\rho' = (1 - \epsilon)\rho + \epsilon\rho_{err}, \quad (\text{C4})$$

in which no errors happen with a probability $(1 - \epsilon)$ and some error happens with a probability ϵ . In complete generality, the eigenvectors of ρ can be different than the eigenvectors of ρ_{err} unless the commutator vanishes $[\rho, \rho_{err}] = 0$. A typical example for a vanishing commutator is the single-qubit depolarising channel in a single qubit systems, in which case $\rho' = (1 - \epsilon)\rho + \epsilon\text{Id}$ and indeed $[\rho, \text{Id}] = 0$. However, for more than 1 quits (or non-separable states) the above expression does not hold and even single qubit depolarising can introduce a coherent mismatch such that the dominant eigenvector of ρ' is $\sqrt{1-c}|\psi\rangle + \sqrt{c}|\psi_{err}\rangle$.

The coherent mismatch due to incoherent errors is expected to be very small in practically relevant scenarios since the high entropy of the error probabilities from Eq. (1) ensures us that $\|[\rho, \rho_{err}]\| \approx 0$ (i.e., ρ is close to a rank-1 operator). For example, in our numerical simulations in Fig. 2 the infidelity of the largest eigenvector with respect to the pure state obtained from a noise-free computation was below 10^{-4} .

In general, for a high entropy error distribution in Eq. (1) we obtain the spectral decomposition with $\lambda_k \ll 1$ for $k \geq 2$

$$\rho = \sum_{k=1} \lambda_k |\psi_k\rangle\langle\psi_k|.$$

One can compute the first order (in ϵ) corrections to the eigenvectors of ρ' via the usual perturbative series: the largest eigenvector of ρ' is approximately (up to normalisation)

$$|\psi'_1\rangle \approx |\psi_1\rangle + \sum_{k=2} \frac{\langle\psi_k|\epsilon\rho_{err}|\psi_1\rangle}{\lambda_1 - \lambda_k} |\psi_k\rangle = |\psi_1\rangle + \frac{\epsilon}{\lambda_1} \sum_{k=2} \langle\psi_k|\rho_{err}|\psi_1\rangle |\psi_k\rangle = |\psi_1\rangle + \mathcal{O}(\epsilon),$$

where we have used that $\lambda_1 - \lambda_k \approx \lambda_1$. Indeed the result is bounded due to the norm of the fist order correction $\sum_{k=2} |\langle\psi_k|\rho_{err}|\psi_1\rangle|^2 = |\text{Col}_1[\rho_{err}]|^2 \leq 1$, hence the scaling of the correction $\mathcal{O}(\epsilon)$. Here $\text{Col}_1[\rho_{err}]$ is the column vector of ρ_{err} whose norm is bounded by the largest eigenvalue.

Let us now focus on the repeated application of the noise channel from Eq. (C4) which can be used to model a quantum circuit that applies a series of noisy quantum gates with error probability ϵ . The incoherent decay of the dominant eigenvalue is expected to decay exponentially $(1 - \epsilon)^\nu$. For large systems one needs to implement a large number ν of gates and therefore one requires to have a sufficiently low per-gate error ϵ in order to keep the dominant eigenvalue above a threshold λ_{\min} – and thus keep the sampling costs in Result 2 practical. Since the strength of the coherent mismatch is proportional to the per-gate error rate ϵ , it is expected to decrease when we decrease ϵ . Interestingly, our numerical simulations of the single- and two-qubit depolarising channel suggest that

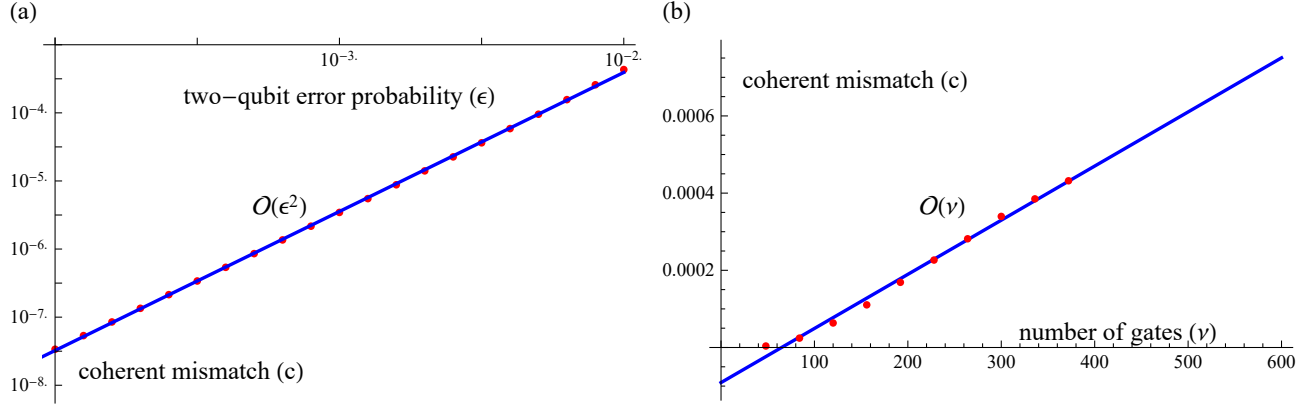


FIG. 4. Coherent mismatch c in the largest eigenvector $\sqrt{1-c}|\psi\rangle + \sqrt{c}|\psi_{err}\rangle$ of the density matrix ρ in case of a purely incoherent noise model (single and two-qubit depolarising). We simulated the same 12-qubit system with 372 noisy gates from Fig. 2 in which single qubit gates undergo single-qubit depolarisation with probability 0.1ϵ while two-qubit gates undergo two-qubit depolarisation with probability ϵ . (a) The coherent mismatch is small and scales with the per-gate error ϵ as $c = \mathcal{O}(\epsilon^2)$ as explained in the text. (b) The coherent mismatch is small and it grows with the number of gates ν at a fixed gate error $\epsilon = 10^{-3}$ as $c = \mathcal{O}(\nu)$.

in the investigated region (see Fig. 4) the coherent mismatch only grows linearly when we increase the number of gates ν . This suggest that when we increase the number of gates the incoherent (exponential) decay of the dominant eigenvalue is significantly more damaging than the (linearly) increasing coherent mismatch.

We illustrate this the following way. Let us define the following quantities. We define the fidelity between the dominant eigenvector $\psi_1^{(\nu)}$ (after the application of ν noisy gates) and the ideal state as $\eta_1 := |\langle \psi_{comp} | \psi_1^{(\nu)} \rangle|^2 = 1 - c$. Furthermore we define the fidelity between the dominant eigenvector and the density matrix ρ as $\eta_2 := \langle \psi_1^{(\nu)} | \rho | \psi_1^{(\nu)} \rangle \approx \lambda$. Here η_1 decays due to the coherent mismatch while $\eta_2 \approx (1 - \epsilon)^\nu$ decays purely due to the incoherent effect of the noise channel. Fig. 4 (a) shows how the ratio η_2/η_1 decreases when we increase the number of gates. Interestingly the scale at which this ratio decays appears to be exponential in the investigated region.

These results suggest that the coherent mismatch in the dominant eigenvector can be expected to be sufficiently small for large, complex quantum circuits. Indeed, these observations are not surprising: we prove elsewhere general upper bounds on the coherent mismatch and prove that it decays exponentially with the entropy of the noise distribution (and quadratically with the largest error probability) [44].

a. Mitigating the coherent mismatch

As discussed in the main text, well-established techniques can be used to mitigate the effect of coherent errors. We now focus on the above introduced coherent mismatch in the eigenvector due to incoherent error channels and demonstrate the effectiveness of an extrapolation approach in Fig. 5 (b). Similarly to Fig. 3 in the main text, we use extrapolation techniques, but here we vary the gate error rate in the state preparation stage (and not in the derangement process). We set gate errors such that two-qubit gates undergo a depolarising noise with probability $\epsilon = 10^{-3}$ and assume that the experimentalist can increase this error in $k = 2, 3, 4, \dots$ steps up to $\epsilon = 10^{-2}$. As expected from the above arguments based on a perturbative expansion of the dominant eigenvector, the measured expectation value should depend on the error levels as a polynomial that has rapidly decaying expansion coefficients due to the fact that the per-gate error level is low as $\epsilon \ll 1$. We have determined extrapolation errors using various fitting techniques as shown in Fig. 5 (b). We define the extrapolation error as the difference between the ideal, error free expectation value $\langle \psi_{comp} | \sigma | \psi_{comp} \rangle$ and the estimated expected value $\frac{\text{Tr}[\rho^n \sigma]}{\text{Tr}[\rho^n]}$ from Method A of Theorem 2. Here $|\psi_{comp}\rangle$ is the state that one would obtain from a perfect, noise-free evaluation of the circuit and in our simulation we consider the same 12-qubit circuit as in Fig. 2 (b) in the main text (refer to Sec. E with $n = 3$ copies).

Indeed, Fig. 5 (b) confirms that the effect of the coherent mismatch can be straightforwardly mitigated by fitting low-order polynomials to the experimental data. The red horizontal line represents the error bound from Result 1 and one can demonstrably suppress the effect of the coherent mismatch below this error bound. As expected, when we increase the degree of the fitting polynomial, the error saturates as it reaches the level from Result 1 which we defined for the case when the coherent mismatch is neglected – and the errors could only be further suppressed by

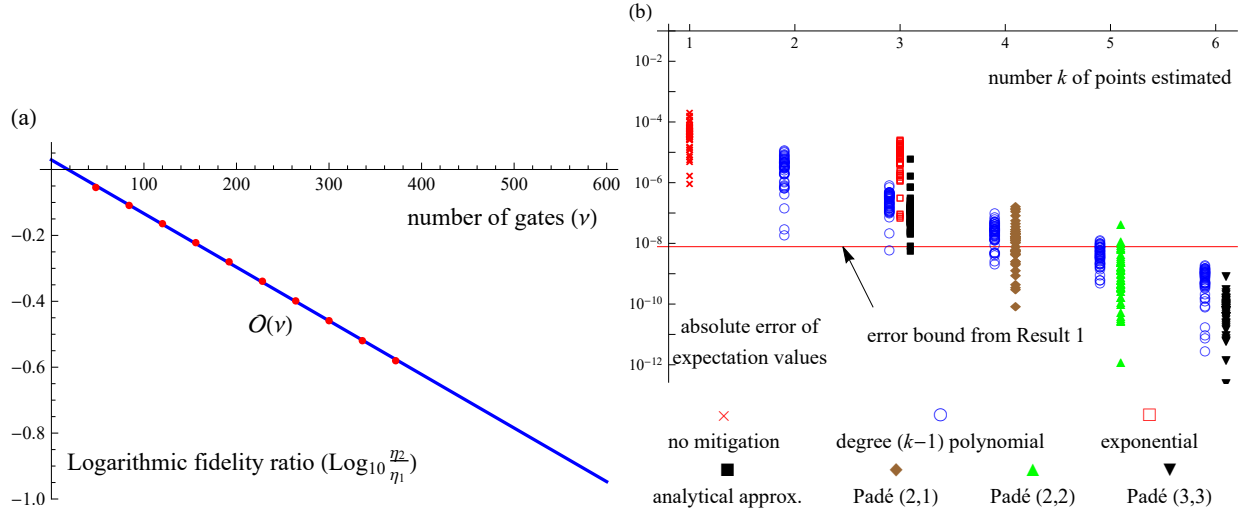


FIG. 5. (a) The fidelity η_1 decreases purely due to the coherent mismatch while the fidelity η_2 decays purely due to the incoherent effect of the noise channel as discussed in Sec. C 1. The ratio η_2/η_1 appears to decay exponentially in the investigated region (linear in the logarithmic plot) when we increase the number of gates for the fixed two-qubit gate error $\epsilon = 10^{-2}$ and this ensures us that the coherent mismatch in the dominant eigenvector becomes negligible for large systems (large ν). We simulated the same circuit as in Fig. 4 (b). (b) Mitigating the error caused by a coherent mismatch in the dominant eigenvector of the density matrix as discussed in Sec. C 1. Gate error levels in the state preparation stage were varied in $k = 2, 3, 4, \dots$ steps and the obtained expectation values were extrapolated to the zero error limit. The red horizontal line represents the error bound from Result 1 and one can straightforwardly suppress the effect of the coherent mismatch below this error bound by fitting low-order polynomials. The error saturates when increasing the degree of the fitting polynomial and can only be further reduced by increasing the number n of copies.

increasing the number n of copies.

Appendix D: Noise resilience of derangements and error extrapolation

Example 3. We now show examples why the derangement operator is highly resilient to errors. We proceed by recapitulating that quantum channels can be represented by a set of non-unique Kraus maps and, in particular, we consider the decomposition into the following sum of unitary transformations as

$$\rho' = (1 - \epsilon)U\rho U^\dagger + \epsilon \sum_m c_m U_m \rho U_m^\dagger,$$

where U is the ideal unitary transformation, $\sum_k c_m = 1$ and $0 \leq \epsilon, c_m \leq 1$, while the erroneous Kraus operators are unitary via $U_m U_m^\dagger = \text{Id}$. The deviation from the ideal transformation can be interpreted as unitary transformations that randomly affect the eigenvectors $|\psi\rangle$ of the quantum state as $U_m|\psi\rangle$ with probability ϵc_m .

Let us now analyse how such errors affect our procedure when they occur during the derangement operator, i.e., we set the ideal transformation U to be our derangement circuit from Fig. 1. First, we show that the orthogonality relations in the proof of Theorem 1 are resilient to such noise events. In particular, recall that the derangement operator symmetrises the input state as, e.g.,

$$D_n|\psi_1, \psi_2, \dots, \psi_n\rangle = |\psi_n, \psi_1, \dots, \psi_{n-1}\rangle,$$

which would ideally ensure that only permutation-symmetric combinations contribute the output via the orthogonality relation from Eq. (A4) as

$$\langle \psi_{k_1}, \psi_{k_2}, \dots, \psi_{k_n} | \sigma \psi_{k_n}, \psi_{k_1}, \dots, \psi_{k_{n-1}} \rangle = \langle \psi_{k_1} | \sigma \psi_{k_n} \rangle \langle \psi_{k_2} | \psi_{k_1} \rangle \cdots \langle \psi_{k_n} | \psi_{k_{n-1}} \rangle.$$

One can show that even if errors occur during the derangement procedure the orthogonality relations are still preserved as

$$\langle U_1 \psi_{k_1}, U_2 \psi_{k_2}, \dots, U_n \psi_{k_n} | \sigma U_1 \psi_{k_n}, U_2 \psi_{k_1}, \dots, U_n \psi_{k_{n-1}} \rangle = \langle U_1 \psi_{k_1} | \sigma U_1 \psi_{k_n} \rangle \langle \psi_{k_2} | \psi_{k_1} \rangle \cdots \langle \psi_{k_n} | \psi_{k_{n-1}} \rangle.$$

It follows that the non-symmetric combinations of input states do not contribute to the output even when the derangement operator is affected by random errors. Note that even though the errors do not directly contribute to the final output (as shown above), the probability that the circuit outputs an error-free result is decreased via the $1 - \epsilon$ factor. This is, however, a trivial effect that only attenuates the output probabilities linearly and can be completely corrected by a linear extrapolation (i.e., estimating the output probabilities at different ϵ values and then extrapolating to $\epsilon = 0$).

Second, let us show that for symmetric input states $|\psi, \psi, \dots, \psi\rangle$ all random errors during the derangement procedure cancel that do not effect the ancilla qubit nor the register to which the observable σ is applied. In fact, we just modify the above equation by not allowing errors on register 1 as

$$\langle \psi, U_2 \psi, \dots, U_n \psi | \sigma \psi, U_2 \psi, \dots, U_n \psi \rangle = \langle \psi | \sigma \psi \rangle \langle \psi | \psi \rangle \cdots \langle \psi | \psi \rangle = \langle \psi | \sigma | \psi \rangle.$$

The second equation shows that we obtain the correct contribution despite all registers (except for register 1) has undergone some random error U_2, U_3 etc. Our previous argument again holds: despite these error events do not directly contribute to the final output of the circuit, the probability of an error-free output is attenuated linearly which, nonetheless, can be completely corrected by a linear extrapolation.

In summary, the derangement measurement is highly resilient to errors and completely protects the permutation symmetry of input states even when the derangement operator suffers from experimental noise. However, errors that affect the qubits to which the observable σ is applied will degrade the final result *non-trivially* via $\langle U_1 \psi | \sigma | U_1 \psi \rangle$, where U_1 is some unitary noise process that occurs with a (possibly) low probability. Nevertheless, we show in the main text and in the following theorem that these erroneous contributions can be successfully mitigated with, e.g., extrapolation techniques.

Theorem 3. *Assume that a circuit consists of a sequence of ν noisy quantum gates, and each gate's error model is of the form $(1 - \epsilon)\Phi_k + \epsilon\mathcal{E}_k$, where Φ_k is the ideal, error-free quantum channel and \mathcal{E}_k is an arbitrary error channel (CPTP map) that occurs with probability ϵ . Most typical error models are of this form, including dephasing, depolarising, inhomogeneous Pauli errors, arbitrary unital channels and beyond (\mathcal{E}_k need not be local or two-local). In a circuit that consists of number ν such gates, any expectation value E will depend on the error probability ϵ as a degree ν polynomial via*

$$E(\epsilon) = E_0 + \sum_{k=1}^{\nu} \epsilon^k E_k,$$

where E_k are real polynomial coefficients. One can therefore exactly determine the ideal expectation value $E(0)$ by estimating $E(\epsilon)$ at $\nu+1$ points in ϵ . The so-called Lagrange polynomial or the Newton polynomial provide explicit formulas for computing $E(\epsilon)$ from the pointwise reconstructions $E(\epsilon_k)$. Furthermore, one can approximate the dependence on ϵ via, e.g., the (3,3) Padé approximation as

$$E(\epsilon) \approx E_0 - \tilde{\eta}\epsilon \frac{(1-\epsilon)^\nu}{2\epsilon-1} \approx \frac{a_1\epsilon + a_2\epsilon^2 + a_3\epsilon^3}{1 + a_4\epsilon + a_5\epsilon^2}, \quad (\text{D1})$$

that only requires the coefficients a_1, a_2, a_3, a_4, a_5 to be fitted to experimental data.

Proof. Applying ν gates in a sequence will result in the product of channels

$$\prod_{k=1}^{\nu} [(1-\epsilon)\Phi_k + \epsilon\mathcal{E}_k] = (1-\epsilon)^\nu \prod_{k=1}^{\nu} \Phi_k + \sum_{k=1}^{\nu} (1-\epsilon)^{\nu-k} \epsilon^k \mathcal{G}_k, \quad (\text{D2})$$

where \mathcal{G}_k is a channel which decomposes into the sum of all terms in which k errors occur and $\prod_{k=1}^{\nu} \Phi_k$ is the ideal error-free circuit. We can introduce the circuit with no errors as $\mathcal{G}_0 := \prod_{k=1}^{\nu} \Phi_k$ which simplifies our formula as.

$$\prod_{k=1}^{\nu} [(1-\epsilon)\Phi_k + \epsilon\mathcal{E}_k] = \sum_{k=0}^{\nu} (1-\epsilon)^{\nu-k} \epsilon^k \mathcal{G}_k, \quad (\text{D3})$$

It follows that any expectation value (with respect to some observable \mathcal{H}) will be of the form

$$E = \text{Tr}\{\mathcal{H} \prod_{k=1}^{\nu} [(1-\epsilon)\Phi_k + \epsilon\mathcal{E}_k] \rho\} = \sum_{k=0}^{\nu} (1-\epsilon)^{\nu-k} \epsilon^k \text{Tr}\{\mathcal{H} \mathcal{G}_k \rho\}, \quad (\text{D4})$$

therefore any expectation value can be expressed as a degree ν polynomial as a function of the error probability as

$$E(\epsilon) = E_0 + \sum_{k=1}^{\nu} \epsilon^k E_k, \quad (\text{D5})$$

where E_0 is the ideal, noise-free expectation value and E_k are polynomial coefficients.

Let us now write (without loss of generality) that the expectation values are of the form $\text{Tr}\{\mathcal{H} \mathcal{G}_k \rho\} = \tilde{\eta} + \eta_k$, where $\tilde{\eta}$ is a mean value and η_k expresses the deviation from the mean value. Let us assume that $\eta_k \ll \tilde{\eta}$, which in the case of the derangement operator is motivated by our argument in 3, that most errors do not contribute and therefore $\tilde{\eta} \approx 0$. In this case we can evaluate the summation analytically for the mean value

$$E(\epsilon) = E_0 + \sum_{k=1}^{\nu} (1-\epsilon)^{\nu-k} \epsilon^k \text{Tr}\{\mathcal{H} \mathcal{G}_k \rho\} = E_0 + \tilde{\eta} \sum_{k=0}^{\nu} (1-\epsilon)^{\nu-k} \epsilon^k + \mathcal{O}(\eta_k) = E_0 + \tilde{\eta}\epsilon \frac{\epsilon^\nu - (1-\epsilon)^\nu}{2\epsilon-1} + \mathcal{O}(\eta_k). \quad (\text{D6})$$

We can obtain a Padé expansion of the above result at $\epsilon \approx 0$ by neglecting the term ϵ^ν . For example the (3,3) Padé approximation follows as

$$E(\epsilon) \approx E_0 - \tilde{\eta}\epsilon \frac{(1-\epsilon)^\nu}{2\epsilon-1} \approx E_0 - \tilde{\eta} \frac{\epsilon + a(n)\epsilon^2 + b(n)\epsilon^3}{1 + c(n)\epsilon + d(n)\epsilon^2}, \quad (\text{D7})$$

where $a(n), b(n), c(n), d(n)$ are the Padé expansion coefficients that depend on the number n of gates ν , for example

$$a(n) = \frac{2(62 + 11n - 8n^2 + n^3)}{5(26 - 9n + n^2)}. \quad (\text{D8})$$

Indeed this expansion is only valid when $\eta_k \approx 0$. Nevertheless, we propose to approximate the polynomial

$$E(\epsilon) \approx \frac{a_1\epsilon + a_2\epsilon^2 + a_3\epsilon^3}{1 + a_4\epsilon + a_5\epsilon^2}, \quad (\text{D9})$$

by fitting the coefficients a_1, a_2, a_3, a_4, a_5 to experimental data. \square

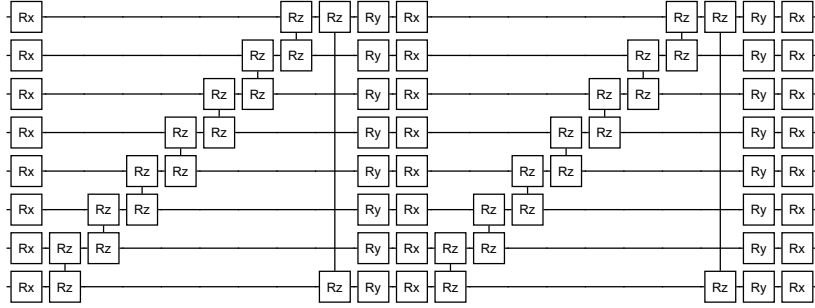


FIG. 6. Example of a 2-block ansatz circuit of 8 qubits. We used a 10-block circuit of 12 qubits in our simulations in Fig. 2 consisting of overall 372 noisy gates. Each two-qubit gate undergoes 2-qubit depolarising noise with 0.5% probability and each single-qubit gate undergoes depolarising noise with 0.05% probability.

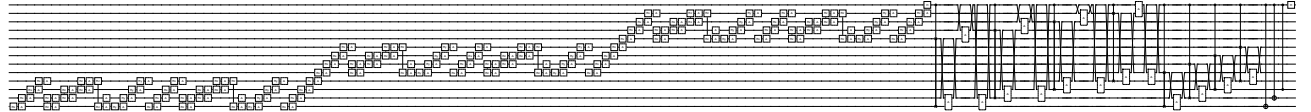


FIG. 7. Circuit that we simulate in Fig. 3. A controlled SWAP gate acting on qubits k, l and m are followed by two qubit depolarisations between qubits k, l and k, m and l, m . A variant in which damping errors follow the depolarisations effectively resulted in the same error mitigation performance.

Appendix E: Numerical Simulations

1. Simulations in Fig. 2

We consider an alternating-layer ansatz with 10 layers and 12 qubits as illustrated in Fig. 6. The circuit consists of overall 372 noisy gates and each two-qubit gate undergoes 2-qubit depolarising noise with 0.5% probability while each single-qubit gate undergoes depolarising noise with 0.05% probability. Each gate is parametrised and we have selected their parameters randomly.

We computed the density matrix of a single copy of the state ρ and our derangement circuit uses n copies of this state as input. While we have numerically verified full derangement circuits with smaller density matrices, here we aim to efficiently compute approximation errors. In particular, we only need to store a single copy of ρ and perform computations to obtain $\text{Tr}[\rho^n \sigma]$ and $\text{Tr}[\rho^n]$ for randomly selected Pauli strings σ . Furthermore, we diagonalise ρ and use its eigenvalues for computing Rényi entropies exactly while we use its dominant eigenvector $|\psi\rangle$ to determine the ‘ideal’ expectation value $\langle\psi|\sigma|\psi\rangle$.

We remark here that we compute approximation errors as the deviation from the expectation value obtained from the dominant eigenvector $\langle\psi|\sigma|\psi\rangle$ and do not directly compare to noise-free computations due to the coherent mismatch discussed in Sec. C 1 (which becomes negligible for large systems and can be addressed with standard techniques). In our simulations this coherent mismatch was below 10^{-4} , and could be corrected with usual techniques that aim to suppress coherent errors as discussed in the main text.

2. Simulations in Fig. 3

We have simulated a derangement circuit that takes $n = 3$ copies of a noisy 4-qubit state as input and the controlled SWAP operators also undergo depolarising noise (with a probability of 10^{-3}) as shown in Fig. 7. The input state is produced by a parametrised 4-qubit circuit and we have selected 50 sets of parameters randomly and performed extrapolation techniques on each instance as shown in Fig. 3.